AD-A272 973

‖‖‖‖‖‖‖‖‖‖‖‖‖‖‖‖‖‖
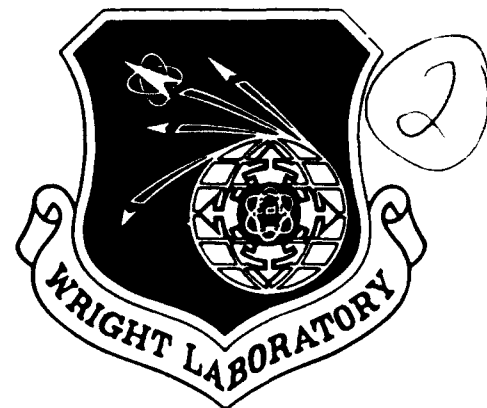
WL-TR-93-3080

Characteristic Based Methods for the Time-Domain Maxwell Equations

J. S. Shang

August 1993

Final Report for Period: June 1990-February 1991

Approved for public release; distribution is unlimited

DTIC
S ELECTE
NOV 22 1993
A

AVIONICS DIRECTORATE
WRIGHT LABORATORY
AIR FORCE MATERIEL COMMAND
WRIGHT PATTERSON AFB OH 45433-7409

93-28376
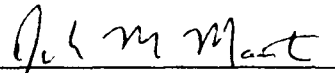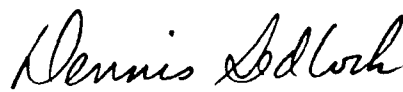‖‖‖‖‖‖‖‖‖‖‖‖‖‖‖‖‖‖

93 11 19 003

NOTICE

When Government drawings, specifications, or other data are used for any purpose other than in connection with a definitely Government-related procurement, the United States Government incurs no responsibility or any obligation whatsoever. The fact that the government may have formulated or in any way supplied the said drawings, specifications, or other data, is not to be regarded by implication, or otherwise in any manner construed, as licensing the holder, or any other person or corporation; or as conveying any rights or permission to manufacture, use, or sell any patented invention that may in any way be related thereto.

This report is releasable to the National Technical Information Service (NTIS). AT NTIS, it will be available to the general public, including foreign nations.

This technical report has been reviewed and is approved for publication.

W. PHILLIP WEBSTER
Technical Manager
CFD Research Section

JOSEPH M. MANTER
Chief
CFD Research Branch

DENNIS SEDLOCK
Actg Chief
Aeromechanics Division

If your address has changed, if you wish to be removed from our mailing list, or if the addressee is no longer employed by your organization please notify WL/FIMC, WPAFB, OH 45433-7562 to help us maintain a current mailing list.

Copies of this report should not be returned unless return is required by security considerations, contractual obligations, or notice on a specific document.

REPORT DOCUMENTATION PAGE

Public reporting burden for this collection of information is estimated to average 1 hour per response, including the time for reviewing instructions, searching existing data sources, gathering and maintaining the data needed, and completing and reviewing the collection of information. Send comments regarding this burden estimate or any other aspect of this collection of information, including suggestions for reducing this burden, to Washington Headquarters Services, Directorate for Information Operations and Reports, 1215 Jefferson Davis Highway, Suite 1204, Arlington, VA 22202-4302, and to the Office of Management and Budget, Paperwork Reduction Project (0704-0188), Washington, DC 20503

1. AGENCY USE ONLY (Leave blank)	2. REPORT DATE 9 Aug 93	3. REPORT TYPE AND DATES COVERED Final Report, Jun 90 - Feb 91

4. TITLE AND SUBTITLE Characteristic Based Methods for the Time-Domain Maxwell Equations	5. FUNDING NUMBERS RE: 61102F PR: 2307 TA: N6 WU: 11
6. AUTHOR(S) J. S. Shang	

7. PERFORMING ORGANIZATION NAME(S) AND ADDRESS(ES) Flight Dynamics Directorate Wright Laboratory Air Force Materiel Command Wright-Patterson AFB OH 45433-7562	8. PERFORMING ORGANIZATION REPORT NUMBER WL-TR-93-3080

9. SPONSORING / MONITORING AGENCY NAME(S) AND ADDRESS(ES) Flight Dynamics Directorate Wright Laboratory Air Force Materiel Command Wright-Patterson AFB OH 45344-7562	10. SPONSORING / MONITORING AGENCY REPORT NUMBER WL-TR-93-3080

11. SUPPLEMENTARY NOTES

12a. DISTRIBUTION / AVAILABILITY STATEMENT Approved for public release; unlimited distribution	12b. DISTRIBUTION CODE

13. ABSTRACT (Maximum 200 words)

Numerical procedures for solving the time-domain Maxwell equations based on the theory of characteristics were successfully developed. Both explicit and implicit methods were formulated by the time-central and spatial-windward algorithm to better describe wave motion. A new trapezoidal consistent implicit scheme was shown to be unconditionally stable for the linear initial value system and was able to generate numerical solutions comparable to those of the established explicit method. The formulation of the three-dimensional system including generalized coordinate system was completed but not explored. The present 2-D results on Cartesian frame demonstrated a potential for numerical efficiency improvement.

14. SUBJECT TERMS Time-domain Maxwell Equation, Trapezoidal Consistent Implicit Scheme, Cartesian Frame	15. NUMBER OF PAGES 49
	16. PRICE CODE

17. SECURITY CLASSIFICATION OF REPORT Unclassified	18. SECURITY CLASSIFICATION OF THIS PAGE Unclassified	19. SECURITY CLASSIFICATION OF ABSTRACT Unclassified	20. LIMITATION OF ABSTRACT Unlimited

Contents

Accesion For		
NTIS CRA&I		☑
DTIC TAB		☐
Unannounced		☐
Justification		
By		
Distribution /		
Availability Codes		
Dist	Avail and / or Special	
A-1		

iii

List of Figures

List of Tables

Acknowledgements

1. Introduction

The current interest in hypersonic flows invigorates the interdisciplinary research of chemical kinetics and aerodynamics. Significant progress has been made in simulating the nonequilibrium dissociation phenomenon for high temperature air associated with hypersonic flight[1,2,3,4]. When the energy level of a gaseous medium reaches an even higher excited state, the gas atoms ionize. The moving charged particles of the ionized gas mixture, will in turn, create an electromagnetic field and introduce an additional diffusion process for energy transfer[5]. A seemingly unrelated current interest in radar cross-section reduction research also receives considerable attention[6,7,8]. In this scientific discipline, a major portion of the effort must concentrate on analyzing the scattering or reflecting of waves in an electromagnetic field[9,10,11]. In this sense, the two entirely different areas of research have a common interest, namely to acquire a better analytical capability for the electromagnetic field.

Both the forced diffusion of an ionized heterogeneous gaseous mixture and the scattering and emission of electromagnetic waves from radiating bodies can be described by the time-dependent Maxwell equations. The system of partial differential equations is hyperbolic and is an initial-value problem[12]. Since the eigenvalues of the system of equations are real, the values along two intersecting characteristics determine the solution everywhere, and any discontinuities of a given solution would be continued into the interior domain. For all finite-difference time-domain approximations of the Maxwell equations, a fundamental dilemma arises from the necessity to impose boundary conditions on a finite spatial domain to an initial-value problem. In addition to the possible degradation of the numerical solution accuracy of the interacting incident and scattering wave patterns, the reflecting waves from the artificial boundaries lead to erroneous accumulations of energy in the computational domain, leading, in turn, to unrealistic modulations of the wave amplitude[7,11]. Numerous

1

approximations over the years have been developed to overcome this dilemma[13,14,15]. The most frequently adopted numerical procedure is probably that of Enquist and Majda[14,15]. In their approach, the unbounded surrounding at the artificial boundaries is simulated by using absorbing boundary conditions. In spite of its successful applications, the approximate boundary condition, however, still is inherently limited as applied to the total field[15]. Another pacing item arising from numerical simulations of the radar signature analysis is an urgently needed improvement in numerical efficiency[6,7,8,9,10]. For wave propagation phenomenon, the adequate numerical resolution of wave packets at a given frequency is dictated by the minimal wave number within the frequency range. At an extremely high frequency, e.g., gigahertz range, the required number of discretized data nodes to solve a practical engineering problem is enormous[6,7]. The aggregated consequence is that large amounts of data are to be processed, usually by a conditionally stable numerical algorithm, which limits our capability in this area of scientific endeavor. A possible alternative may be derived from the recent advances in flux-splitting schemes for solving the Euler equations in computational fluid dynamics (CFD).[16,17,18,19,20,21]

The fundamental idea of flux-splitting methods in solving hyperbolic systems of equations is based on the eigenvalue analysis[16,17,18]. In finite-difference approximations, the well-posedness requirement and the numerical stability of the solving scheme are ultimately linked to eigenvalues of the governing equations[22,23]. The most recent progress in characteristic based and the total variation diminishing (TVD) schemes[24,25] demonstrate that numerical stability and accuracy can be drastically improved by using an appropriate finite differencing for split flux vectors according to the signs of the eigenvalues. In essence, the system of equations is manipulated to achieve the Riemann problem[26]. For the electromagnetic field of radar signature analysis, the main concern is the appropriate treatment of incident and scattering wave propagation from a reflecting body. Thus, the elimination of nonphysical reflecting waves from artificial outer boundaries is a paramount concern

2

and could be alleviated by the theory of characteristics[7,15]. The present effort will address this issue by using a newly acquired CFD technique for electromagnetic field calculations. The approach to numerical efficiency improvement is also based on the uncoupled eigenvector structure and the introduction of suitable implicit algorithms to solve the Maxwell equations.

The flux-splitting technique, however, has an inherent limitation in that the coefficient matrices of the governing equations when written in flux vector form can be diagonalized in only one dimension at a time[16,17,18]. Therefore, in multidimensional analysis, the exact no-reflection farfield wave condition is achievable only for wave motion which possesses a dominant orientation. In principle, this favorable condition is attainable by casting the Maxwell equations in general curvilinear coordinates. On the artificial farfield boundary, the coordinate will be adapted to align with the principal axis of the wave propagation to eliminate or at least to minimize undesirable wave reflection. On the interface of dielectric media of different permittivities, the complex scattering shape will be prescribed by a body conformal coordinate surface. The surface outward normal, required by the boundary relationships of the electromagnetic fields[11], can be easily computed.

In summary, the present investigation attempts to develop efficient numerical procedures for solving the time-dependent Maxwell equations in free space. The electric flux density and the magnetic flux density will be transformed by a diagonalizing matrix to acquire invariants along the respective characteristics. The split and uncoupled flux vectors will then be solved by second-order temporal and spatially windward finite-difference approximations.

2. Analysis

Maxwell's equations for the electromagnetic field in free space can be written in flux vector form in a Cartesian frame as[11]

$$\frac{\partial \overline{U}}{\partial t} + \frac{\partial \overline{F}}{\partial \overline{U}}\frac{\partial \overline{U}}{\partial x} + \frac{\partial \overline{G}}{\partial \overline{U}}\frac{\partial \overline{U}}{\partial y} + \frac{\partial \overline{H}}{\partial \overline{U}}\frac{\partial \overline{U}}{\partial z} = 0 \qquad (2.1)$$

$$\frac{\partial \overline{U}}{\partial t} + \overline{\overline{A}}\frac{\partial \overline{U}}{\partial x} + \overline{\overline{B}}\frac{\partial \overline{U}}{\partial y} + \overline{\overline{C}}\frac{\partial \overline{U}}{\partial z} = 0 \qquad (2.2)$$

Where the coefficient matrices (Jacobian of flux vector) A, B, and C are:

$$\overline{\overline{A}} = \begin{bmatrix} 0 & 0 & 0 & 0 & 0 & 0 \\ 0 & 0 & 0 & 0 & 0 & \frac{1}{\epsilon} \\ 0 & 0 & 0 & 0 & -\frac{1}{\epsilon} & 0 \\ 0 & 0 & 0 & 0 & 0 & 0 \\ 0 & 0 & -\frac{1}{\mu} & 0 & 0 & 0 \\ 0 & \frac{1}{\mu} & 0 & 0 & 0 & 0 \end{bmatrix}$$

$$\overline{\overline{B}} = \begin{bmatrix} 0 & 0 & 0 & 0 & 0 & -\frac{1}{\epsilon} \\ 0 & 0 & 0 & 0 & 0 & 0 \\ 0 & 0 & 0 & \frac{1}{\epsilon} & 0 & 0 \\ 0 & 0 & \frac{1}{\mu} & 0 & 0 & 0 \\ 0 & 0 & 0 & 0 & 0 & 0 \\ -\frac{1}{\mu} & 0 & 0 & 0 & 0 & 0 \end{bmatrix}$$

$$(2.3)$$

1

$$
\overline{\overline{C}} = \begin{bmatrix} 0 & 0 & 0 & 0 & \frac{1}{\epsilon} & 0 \\ 0 & 0 & 0 & -\frac{1}{\epsilon} & 0 & 0 \\ 0 & 0 & 0 & 0 & 0 & 0 \\ 0 & -\frac{1}{\mu} & 0 & 0 & 0 & 0 \\ \frac{1}{\mu} & 0 & 0 & 0 & 0 & 0 \\ 0 & 0 & 0 & 0 & 0 & 0 \end{bmatrix}
$$

$$
\overline{U} = [E_x, E_y, E_z, H_x, H_y, H_z]^t
$$

Where ϵ and μ are the permittivity and permeability which relate the electric flux density to the electric field intensity and magnetic flux density to the magnetic field intensity respectively.

The eigenvalues of the coefficient matrices $\overline{\overline{A}}$, $\overline{\overline{B}}$, and $\overline{\overline{C}}$ are identical, and unfortunately contain multiplicities. Care must be exercised to ensure that all associated eigenvectors are linearly independent.

$$
\lambda = \left\{ +\frac{1}{\sqrt{\epsilon\mu}}, -\frac{1}{\sqrt{\epsilon\mu}}, 0, +\frac{1}{\sqrt{\epsilon\mu}}, -\frac{1}{\sqrt{\epsilon\mu}}, 0 \right\} \tag{2.1}
$$

However, linear independent eigenvectors associated with each eigenvalue still can be found by reducing the matrix equation,$(\overline{\overline{A}} - \overline{\overline{I}}\lambda)\overline{X} = 0$, to the Jordan normal form.

According to matrix theory, if the coefficient matrix $\overline{\overline{A}}$ (or $\overline{\overline{B}}$ or $\overline{\overline{C}}$) can be diagonalized, then there exists a nonsingular matrix $\overline{\overline{S}}$ such that

$$
\overline{\overline{D}}_\lambda = \overline{\overline{S}}^{-1}\overline{\overline{AS}} \tag{2.5}
$$

The columns of $\overline{\overline{S}}$ are simply the eigenvectors of the coefficient matrix $\overline{\overline{A}}$.

The multidimensional Maxwell equations are separated into one-dimensional components in each direction of the Cartesian frame. For the present investigation and without loss of generality, the scattered waves are considered to be confined in isotropic media separated by physical interface. Under these conditions, the permittivity and permeability are assumed

to have constant values[11]. Therefore, the left-hand inverse of the similarity transformation matrix $\overline{\overline{S}}$ can be brought into the differentiation with respect to both time and space. The resulting equations indicate that along trajectories with slopes of positive and negative speed of light, and with zero eigenvalue, the characteristic variables are invariant. Most importantly for the system of equations, all transformed dependent variables are completely uncoupled and can be solved individually. In other words, the matrix system is decomposed into upper and lower tridiagonal structures. Only a single sweep will be required to solve the complete system of discretized equations. For an implicit solving scheme, the pentadiagonal inversion procedure becomes unnecessary and leads to a very efficient numerical procedure.

$$\frac{\partial \overline{W}}{\partial t} + \lambda \frac{\partial \overline{W}}{\partial x} = 0 \tag{2.6}$$

$$\overline{W} = \overline{W}(w_1, w_2, w_3, w_4, w_5, w_6)$$

λ	$\overline{W} = \overline{\overline{S}}^{-1}\overline{U}$
$\frac{1}{\sqrt{\epsilon\mu}}$	$\frac{1}{2}\left(\sqrt{\frac{\epsilon}{\mu}}E_z - H_y\right)$
$-\frac{1}{\sqrt{\epsilon\mu}}$	$\frac{1}{2}\left(\sqrt{\frac{\epsilon}{\mu}}E_z + H_y\right)$
0	H_x
$\frac{1}{\sqrt{\epsilon\mu}}$	$\frac{1}{2}\left(\sqrt{\frac{\epsilon}{\mu}}E_z + H_x\right)$
$-\frac{1}{\sqrt{\epsilon\mu}}$	$\frac{1}{2}\left(\sqrt{\frac{\epsilon}{\mu}}E_z - H_x\right)$
0	H_y

$$\tag{2.7}$$

Similar expressions for the two other components are found in the identical manner. The multidimensional problem will be solved by either a windward explicit method or an approximate factored implicit scheme[27,28]. A specific selection of numerical algorithms is one of the major research goals. A criterion of the choice is that the algorithm yield low dissipative and dispersive errors. In this connection, numerical schemes which can satisfy the

shift condition in the degenerated one-dimensional setting is sought[27,28,29]. The ease of implementation of boundary conditions on either a scattering body or the outer computational domain is also a major consideration. For a simple wave equation, the preference seems to have been biased toward the explicit windward method by Warming and Beam[6,27]. However, a windward implicit method also possesses this unique property and is included in the present investigation[28].

A critical step here is that the finite differencing is implemented to honor the physical orientation of the wave propagation[7,16,18]. For example, forward and backward differencing of the spatial variables are formed for the negative and the positive eigenvalue respectively. In general, information is propagated from the interior/exterior of the computational domain to the boundary along characteristics[7,18]. The characteristic equations, Eq (6), are really the compatibility relationships and are equally applicable on the boundaries of the computational domain. To use characteristic data to establish the exit wave boundary conditions, knowledge of the orientation of the wave front with respect to the boundary surface becomes essential. A unique feature of the electromagnetic field provides this required information nicely. In free space, the direction of wave propagation is always known since the electromagnetic waves move in the direction perpendicular to both the electric and magnetic fields, $E \times H$[7,11]. Near the outer control surface, the characteristic equations will be projected to the principal axis of the wave motions based on the known local solution. A coordinate transformation from the Cartesian frame to a general curvilinear system can then be adopted to ensure coordinate alignment with wave motion. Another advantage of the coordinate transformation is that it permits a high numerical resolution by local mesh refinement if necessary[23]. Meanwhile, the complex scattering body is easily represented by body conformal coordinates.

A general curvilinear coordinate transformation is introduced by defining a one-to-one relationship between two sets of independent variables. In the present analysis, the coordinate

system is limited to the spatially independent variables.

$$\xi = \xi(x, y, z)$$

$$\eta = \eta(x, y, z)$$

$$\zeta = \zeta(x, y, z)$$

A one-to-one coordinate transformation is ensured through the nonvanishing Jacobian of coordinate transformation. By the chain rule of differentiation, the Maxwell equations acquire the following form, similar to that in the Cartesian system.

$$\frac{\partial \overline{U}}{\partial t} + \overline{\overline{A}}\frac{\partial \overline{U}}{\partial \xi} + \overline{\overline{B}}\frac{\partial \overline{U}}{\partial \eta} + \overline{\overline{C}}\frac{\partial \overline{U}}{\partial \zeta} = 0 \qquad (2.8)$$

The three-dimensional problem is separated into three one-dimensional problems along each transformed coordinate line. For the present purpose, only one component of the Maxwell equations is presented. The other components are nearly identical, differing only in the cyclic rotation of the metrics of coordinate transformation. The eigenvalues of the general curvilinear system are obtained after some algebraic manipulation. As expected, the functional forms are similar for all components in the transformed space and the details will not be presented here.

$$\frac{\partial \overline{W}}{\partial t} + \lambda \frac{\partial \overline{W}}{\partial \xi} = 0 \qquad (2.9)$$

$$\overline{W} = \overline{W}(w_1, w_2, w_3, w_4, w_5, w_6) \qquad (2.10)$$

$$\lambda = \left\{ \sqrt{\frac{\xi_x^2 + \xi_y^2 + \xi_z^2}{\mu\epsilon}}, -\sqrt{\frac{\xi_x^2 + \xi_y^2 + \xi_z^2}{\mu\epsilon}}, 0, \right.$$
$$\left. \sqrt{\frac{\xi_x^2 + \xi_y^2 + \xi_z^2}{\mu\epsilon}}, -\sqrt{\frac{\xi_x^2 + \xi_y^2 + \xi_z^2}{\mu\epsilon}}, 0 \right\} \qquad (2.11)$$

8

Following a similar procedure as used in developing the characteristic equations for the Cartesian system, a typical set of invariants along one coordinate is

$$w_1 = \frac{1}{2}\left[\sqrt{\frac{\epsilon}{\mu}}(\xi_x E_y - \xi_y E_x) - \xi_x \xi_z H_x - \xi_y \xi_z H_y + \left(\xi_x^2 + \xi_y^2\right) H_z\right] \tag{2.12}$$

$$w_2 = \frac{1}{2}\left[\sqrt{\frac{\epsilon}{\mu}}(\xi_z E_x - \xi_x E_z) - \xi_x \xi_y H_x + \left(\xi_x^2 + \xi_z^2\right) H_y - \xi_y \xi_z H_z\right] \tag{2.13}$$

$$w_3 = \frac{1}{2}\left[\sqrt{\frac{\epsilon}{\mu}}(\xi_y E_x - \xi_x E_y) - \xi_x \xi_z H_x - \xi_y \xi_z H_y + \left(\xi_x^2 + \xi_y^2\right) H_z\right] \tag{2.11}$$

$$w_1 = \frac{1}{2}\left[\sqrt{\frac{\epsilon}{\mu}}(\xi_x E_z - \xi_z E_x) - \xi_x \xi_z H_x + \left(\xi_x^2 + \xi_z^2\right) H_y - \xi_y \xi_z H_z\right] \tag{2.15}$$

$$w_5 = \xi_x^2 E_x + \xi_x \xi_y E_y + \xi_x \xi_z E_z \tag{2.16}$$

$$w_6 = \xi_x^2 H_x + \xi_x \xi_y H_y + \xi_x \xi_z H_z \tag{2.17}$$

The numerical solution of the Maxwell equation is obtained in characteristic variables by three differencing operators along transformed coordinate lines. Forward or backward finite-difference approximations are formed according to the sign of the associated eigenvalue. At the present stage of algorithm development, only two-dimensional simulations are attempted to seek confirmation of the basic concept. Test cases consist of incident transverse electric and magnetic waves propagating through a finite computational domain and electromagnetic pulses generated by an electrical current source perpendicular to the plane of wave motions. Although these simulated phenomena are elementary, they pose severely demanding numerical accuracy requirements for describing discontinous wave behavior and yet possess all essential features of a scattering field. Therefore, the physical boundary

9

conditions of a scattering body are not attempted in the present analysis. Under this framework, numerical results reflect the best possible performance of the new numerical procedures in simulating the scattering electromagnetic field.

3. Numerical Methods

Since the Maxwell equations are diagonalized in each spatial direction and compeletely uncoupled in terms of eigenvectors and associated eigenvalues (positive, negative and null), the windward finite difference approximation is used to better describe the physics. The solution procedure for the eigenvector tied to the null eigenvalue (Eqs 6. and 16.17) is trivial. i.e. the unidirection eigenvector is an invariant with respect to time. For a two dimensional problem, only two split flux equations with nonzero eigenvalue are needed to be solved in each coordinate direction. Three second-order temporal and spatial, explicit and implicit numerical schemes are implemented for the present investigation. All the algorithms considered are either based on or related to Warming and Beam's works for solving the Euler equations[27,28].

The two-step upwind explicit method by Warming and Beam[27] has been adapted for solving the Maxwell equations[6]. This explicit scheme has a conditional stability property that restricts the allowable time step by a CFL value of 2 for a one-dimensional problem. The theoretical limit is reduced to a value of $2/\sqrt{3}$ in three-dimensional simulations. In practical applications. the allowable time-step size which is dictated by the minimum grid spacing. can be drastically reduced even more by the thin film partitions of dielectric media.

One-dimensional solutions of this particular scheme satisfy the shift condition[29,30] at a CFL number equal to 1 and 2. Solutions that possess this unique property contain no quasi-physical error and are therfore highly desirable for accurate description of reflected waves in the far field of a scattering problem. In the present formulation. the two-step method can be simplified to a single-step algorithm by substituting the predicted result into the corrector. The resultant finite-difference approximations for the positive and the negative eigenvalue equations acquire the following forms:

$$w^{n+1}(i,j) = w^n(i,j) - \frac{|\lambda|\,\Delta t}{\Delta x}[w^n(i,j) - w^n(i-1,j)] +$$
$$\frac{|\lambda|\,\Delta t}{\Delta x2}\left[\frac{|\lambda|\,\Delta t}{\Delta x} - 1\right][w^n(i,j) - 2w^n(i-1,j) +$$
$$w^n(i-2,j)] \qquad \lambda > 0 \tag{3.1}$$

$$w^{n+1}(i,j) = w^n(i,j) - \frac{|\lambda|\,\Delta t}{\Delta x}[w^n(i,j) - w^n(i+1,j)] +$$
$$\frac{|\lambda|\,\Delta t}{\Delta x2}\left[\frac{|\lambda|\,\Delta t}{\Delta x} - 1\right][w^n(i,j) - 2w^n(i+1,j) +$$
$$w^n(i+2,j)] \qquad \lambda < 0 \tag{3.2}$$

For the multidimensional problem, the cyclic fractional-step sequence and the total sum procedure were included in the present analysis. Numerical solutions generated from both procedures retain second-order accuracy in space and time. There is essentially no disparity between solutions by these two explicit methods, although the fractional-step method requires additional data at the intermediate temporal step. In addition, the numerical efficiency advantage of the fractional-step method over the total sum scheme no longer exists for solving wave equations. Therefore, no further effort was devoted to its evolution at the present time. For the explicit methods, the numerical boundary conditions at outer edges of the computational domain are easily implemented by specifying data of the exact incoming wave component and by enforcing the null value of the eigenvector in the direction of the exiting wave.

Following the development of Warming and Beam's trapezoidal, second-order implicit approximate-factored algorithms for solving the two-dimensional hyperbolic system[28], the finite-difference approximation can be given as the following:

$$\left(I + \frac{1}{2}\lambda\Delta t\frac{\partial}{\partial x}\right)\Delta w_x^* = -\Delta t\left[\lambda\frac{\partial w_x}{\partial x} + S_x^{-1}S_y\lambda\frac{\partial w_y}{\partial y}\right]^n \tag{3.3}$$

$$\left(I + \frac{1}{2}\lambda\Delta t \frac{\partial}{\partial y}\right)\Delta w_{ij}^{n+1} = -\Delta w_{ij}^* \tag{3.1}$$

One notes that during different numerical sweeps, the differencing operators do not act on the same eigenvector. Therefore, after each numerical sweep, the eigenvectors associated with the next spatial orientation need to be updated by the most recent calculation. This is the direct consequence of our inability to simultaneously diagonalize all coefficient matrices of the Maxwell equations. Since relationships linking the eigenvectors and the electromagnetical field variables are explicit and unambiguous, this inconvenience does not impose an inhibiting constraint for further development into three dimensions. On the other hand, the anticipated future generalization to include arbitrary curvilinear coordinates and dielectric media will incur additional errors of linearization[28,30]. In the present investigation, the system of equations is linear by virtue of the facts that all phenomena occur within an isotropic medium and all metrics of coordinate transformation are assigned constant values. Therefore, the similar matrices of diagonalization are independent of space and time and can be brought into the differential operators to complete the formulation. Otherwise, the final characteristic equations can be achieved only after a local linearization process. This is, however, an inherent feature of using implicit methods to solve a nonlinear equation system.

In the original work of Warming and Beam on the construction of implicit factored schemes for hyperbolic systems[28], a trapezoidal formula in time and internally inconsistent windward scheme was established. Internal inconsistency implies that the explicit and implicit differencing for temporal evaluation are unbalanced. The explicit (RHS) differencing is given by a three-point one-sided approximation, whereas the implicit (LHS) differencing is represented by a two-point one-sided approximation. Although the latter difference approximation is first-order, it operates on the increment of characteristics, and as a consequence the resulting scheme is spatially second-order for any fixed ratio of temporal and spatial increments[28]. This implicit scheme is conditionally stable for the trapezoidal formula and

it satisfies the shift condition at CFL equal to 1. The present time-centered and consistent three-point windward scheme is developed from this framework. The point of departure lies in the fact that the governing hyperbolic system of equations is uncoupled by diagonalization. The pentadiagonal coefficient matrix structure of a bidirectional windward differencing approximation is eliminated. In the present split flux implicit formulation, each characteristic equation can be cast into a simple bidiagonal matrix structure and the inversion process is straightforward. The specific equations solved are:

X sweep: For $\lambda > 0$:

$$w_x^*(i,j) = \frac{\left\{ \begin{array}{c} \left[1 - \frac{3}{4}\left(\frac{\lambda \Delta t}{\Delta x}\right) \right] w_x^n(i,j) + \\ \left(\frac{\lambda \Delta t}{\Delta x}\right)\left[w_x^*(i-1,j) + w_x^n(i-1,j) \right] - \\ \frac{1}{4}\left(\frac{\lambda \Delta t}{\Delta x}\right)\left[w_x^*(i-2,j) + w_x^n(i-2,j) \right] - \\ \frac{1}{4}\left(\frac{\lambda \Delta t}{\Delta y}\right)\left[\left(3w_y^+(i,j) - 4w_y^+(i,j-1) + \right. \right. \\ \left. w_y^+(i,j-2) \right) + \left(3w_y^-(i,j) - \right. \\ \left. \left. 4w_y^-(i,j+1) + w_y^-(i,j+2) \right) \right]^n \end{array} \right\}}{\left[1 + \frac{3}{4}\left(\frac{\lambda \Delta t}{\Delta x}\right) \right]}$$
(3.5)

For $\lambda < 0$:

$$w_x^*(i,j) = \frac{\left\{ \begin{array}{c} \left[1 - \frac{3}{4}\left(\frac{\lambda \Delta t}{\Delta x}\right) \right] w_x^n(i,j) + \\ \left(\frac{\lambda \Delta t}{\Delta x}\right)\left[w_x^*(i+1,j) + w_x^n(i+1,j) \right] - \\ \frac{1}{4}\left(\frac{\lambda \Delta t}{\Delta x}\right)\left[w_x^*(i+2,j) + w_x^n(i+2,j) \right] - \\ \frac{1}{4}\left(\frac{\lambda \Delta t}{\Delta y}\right)\left[\left(3w_y^+(i,j) - 4w_y^+(i,j-1) + \right. \right. \\ \left. w_y^+(i,j-2) \right) + \left(3w_y^-(i,j) - \right. \\ \left. \left. 4w_y^-(i,j+1) + w_y^-(i,j+2) \right) \right]^n \end{array} \right\}}{\left[1 + \frac{3}{4}\left(\frac{\lambda \Delta t}{\Delta x}\right) \right]}$$
(3.6)

For $\lambda = 0$:

$$w_x^*(i,j) = w_x^n(i,j) - \frac{1}{2}\left(\frac{\Delta t}{\mu \Delta y}\right)\left[\left(w^+(i,j+1) - \right. \right.$$
$$\left. w^+(i,j-1) \right) + w^-(i,j+1) - w^-(i,j-1) \right]^n$$
(3.7)

14

Y sweep: For $\lambda > 0$:

$$w_y^{n+1}(i,j) = \frac{\left\{ \begin{array}{l} \left[1 + \frac{3}{4}\left(\frac{\lambda \Delta t}{\Delta y}\right)\right] w_y^n(i,j) + \\ \left(\frac{\lambda \Delta t}{\Delta y}\right)\left[w_y^{n+1}(i,j-1) - w_y^n(i,j-1)\right] - \\ \frac{1}{4}\left(\frac{\lambda \Delta t}{\Delta y}\right)\left[3w_y^{n+1}(i,j-2) - w_y^n(i,j-2)+\right] \\ \left[w_y^*(i,j) - w_y^n(i,j)\right] \end{array} \right\}}{\left[1 + \frac{3}{4}\left(\frac{\lambda \Delta t}{\Delta y}\right)\right]} \tag{3.8}$$

For $\lambda < 0$:

$$w_y^{n+1}(i,j) = \frac{\left\{ \begin{array}{l} \left[1 + \frac{3}{4}\left(\frac{\lambda \Delta t}{\Delta y}\right)\right] w_y^n(i,j) + \\ \left(\frac{\lambda \Delta t}{\Delta y}\right)\left[w_y^{n+1}(i,j+1) - w_y^n(i,j+1)\right] - \\ \frac{1}{4}\left(\frac{\lambda \Delta t}{\Delta y}\right)\left[3w_y^{n+1}(i,j+2) - w_y^n(i,j+2)+\right] \\ \left[w_y^*(i,j) - w_y^n(i,j)\right] \end{array} \right\}}{\left[1 + \frac{3}{4}\left(\frac{\lambda \Delta t}{\Delta y}\right)\right]} \tag{3.9}$$

For $\lambda = 0$:

$$w_y^{n+1}(i,j) = w_y^*(i,j) \tag{3.10}$$

In general, the algorithm is unconditionally stable when applied to a simple wave equation, a feature which may be very valuable in improving numerical efficiency for computational techniques in electromagnetics. The elementary stablity analysis of this algorithm is presented by the modulus of amplification factor and the relative phase error in Figures 1 and 2, respectively. The values of modulus are depicted for the range of CFL numbers from 0.75 to 5.0. It is clear that the numerical method is dissipative and the numerical error is diminished monotonically as CFL is increased. On other hand, the relative phase angle exhibits a predominant leading error for CFL values less than unity, then switches to a persistent lagging error for CFL values greater than 2.
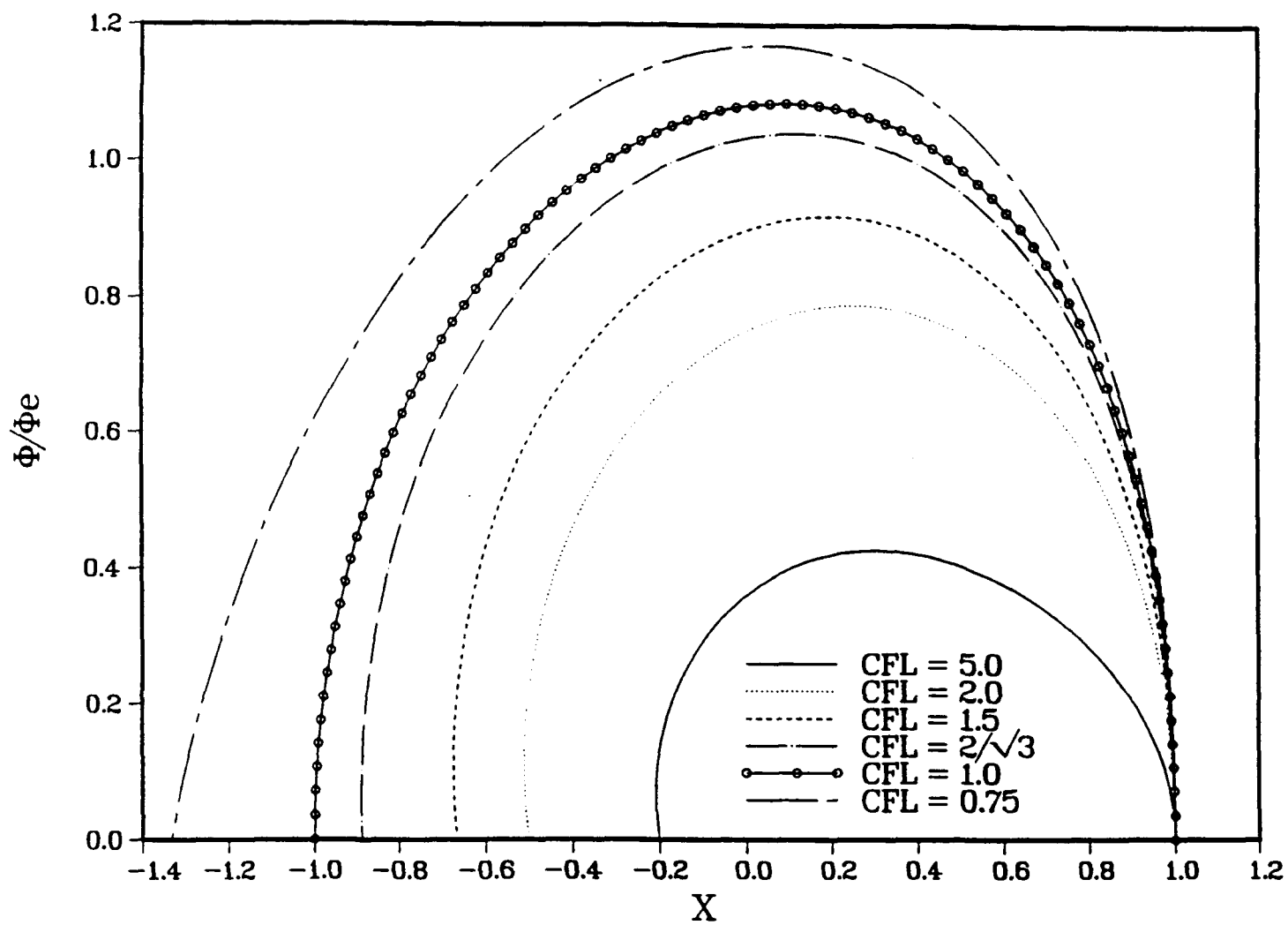
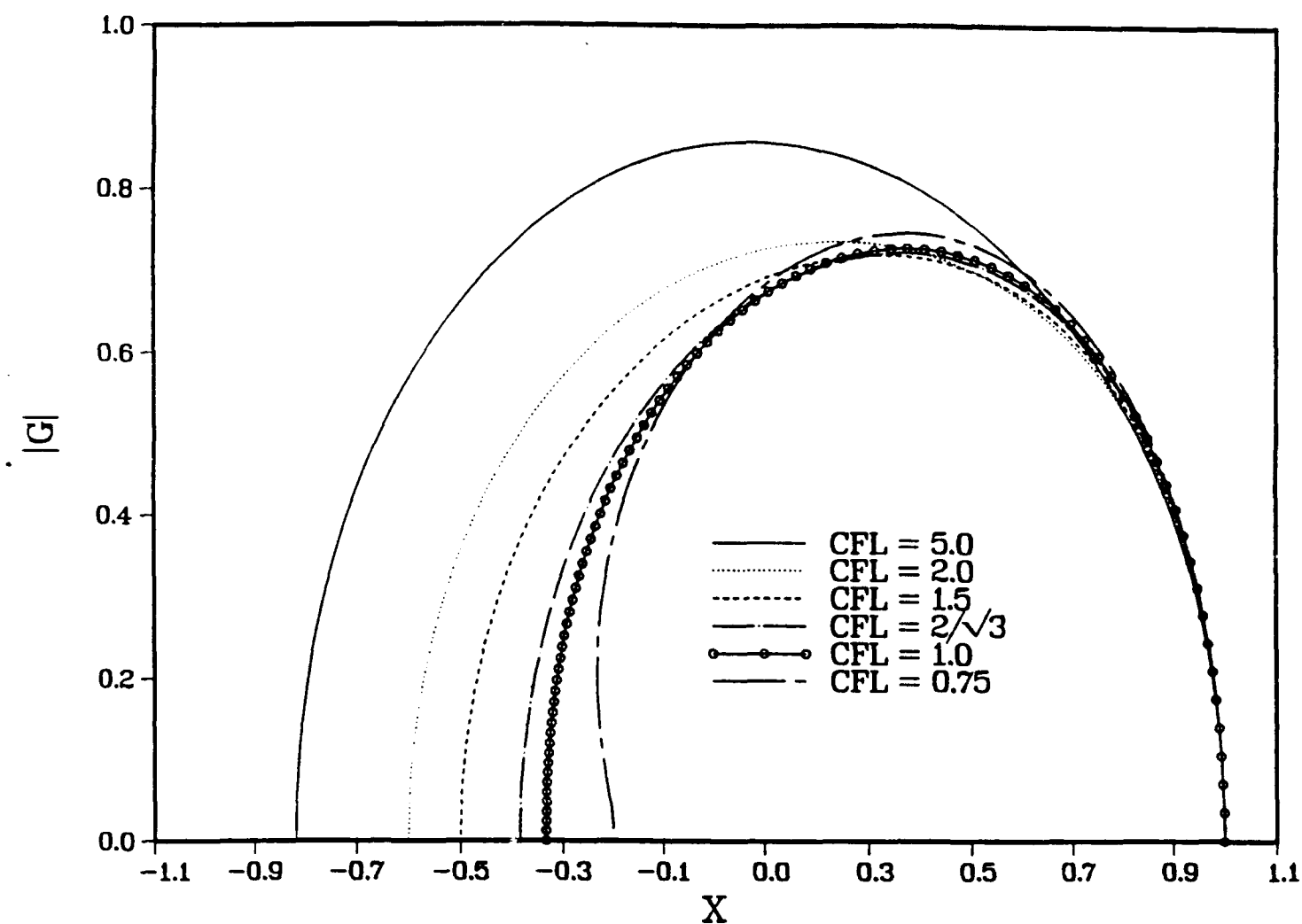Figure 1: Modulus of Amplification Factor $0.75 < CFL < 5.0$

Figure 2: Relative Phase Error $0.75 < CFL < 5.0$

In the range of CFL numbers from 1 to 2, the relative phase angle changes from a slight leading error to a lagging error according to the increasing wave number. The cross-over of relative phase angle from leading to lagging error takes place in the mid-range of wave number and constrains the discrepancy to a relative low magnitude in a wide spectrum. Most importantly, the relative phase error is significantly less than most time- and space-centered implicit schemes in the high wave number domain[28,30].

For the approximate factored implicit scheme, the implementation of numerical boundary conditions at the intermediate time step is more complicated than for the explicit method. In the case when an exact datum at the artificial boundary is known, the intermediate value must be extracted from the next consecutive numerical sweep. That is, the boundary conditions of equations (22), (23), and (24) must be derived from equations (25), (26), and (27) respectively, whereas for the explicit calculations, this issue is completely eliminated by the total sum procedure. For the case where a nonreflecting wave condition is required, the null value of the eigenvector opposite the exiting wave is imposed. Then, any error that may be incurred is contributed by the misalignment of the orientation of wave propagation and the coordinate direction. In principle, this error could be remedied by the coordinate transformation.

4. Discussion of Numerical Results

All numerical results were generated on a 15 × 15 equally-spaced Cartesian system in which metrics of the coordinate transformation assumed a value of either 1 or 0. Thus the linearization error is completely eliminated from the present analysis. Further development of the present methodology for practical applications to include dielectric media and arbitrary scattering bodies will be pursued in upcoming efforts. An IRIS 4D/120 GTX workstation was used exclusively to generate all numerical results. The relative numerical efficiency of all studied numerical procedures is probably best evaluated by the count of arithmetic operations to process the two-dimensional field data.

It is obvious that the upwind explicit method requires the fewest arithmetical operations to complete a field point calculation. However, the trapezoidal, consistent implicit method has no imposed restriction from the stability condition and can process data at far greater time steps. This favorable numerical feature will be ever more apparent when the dielectric media are separated by a thin coating and the time step allowed is controlled by the smallest spatial dimension. Supported by a suitable mesh system for required numerical resolution, the trapezoidal consistent implicit method could have a much higher numerical efficiency than most procedures currently in use[6,7,8,9,10].

Table 1: Arithmetical Operational Count of Numerical Schemes

Basic algorithm	Arithmetical Operational counts
Single-step Upwind, Explicit	52
Trapezoidal, Inconsistent Implicit	78
Trapezoidal, Consistent Implicit	103

Numerical results consist of three groups. First a series of one dimensional wave motion calculations for all three numerical methods at a range of CFL values from 0.75 to 2.0 is presented. Numerical results of explicit and implicit methods are investigated for their ability to accomodate the propagation of a piecewise continous disturbance and to quantify quasi-physical errors. In the second group of results, transverse waves traveling obliquely across orthogonal two dimensional coordinates are presented. The numerical schemes are examined for sensitivity of computed wave structure relative to the imposed boundary conditions. Finally, the new numerical methods are applied to simulate a locally nonanalytical outward propagating electromagnetic field generated by an electric current perpendicular to the plane of transverse waves. In this group of results, the combined effects of a singular perturbation and its outward propagation through a finite compuational domain are delineated.

In Figure 3, the exact electrical field density of a traveling wave is compared with numerical results from the trapezoidal consistent implicit (TCI) and the single-step upwind explicit (SUE) schemes at the CFL value of 2. This is also the maximum allowable time step that can be specified for the SUE method. The solutions are presented at instances when a right-running wave front reaches the mid-point of the computational domain (Fig. 3a) and exits the numerical boundary respectively (Fig 3b). The shift property of the solution by the SUE scheme indicates a perfect translation of the initial value in space. The discontinuous incoming wave front is captured precisely by the SUE method but not by the TCI scheme. When the impulse wave front moves through the computational domain, the SUE method duplicates the exact solution at each and every discretized point (Fig 3a). This highly desirable property of a numerical solution is not preserved for general two-dimensional computations. In contrast, the solution of TCI scheme yielded an 8.4-percent maximum discrepancy from the exact solution.

In spite of the fact that the TCI method has no theoretical stability limit on the time
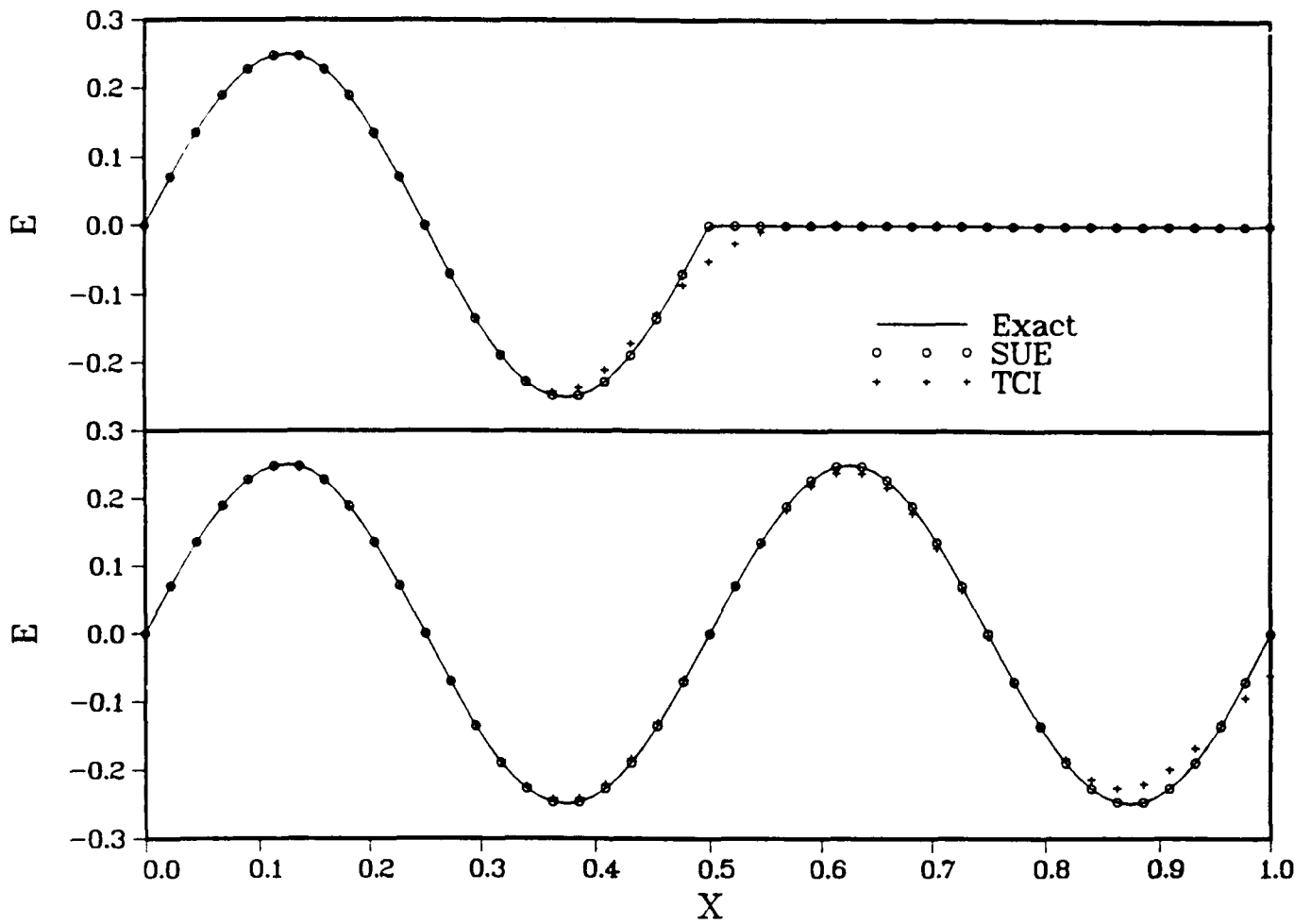
Figure 3: Electrical Field Intensity $CFL = 2.0$

step. the numerical accuracy is controlled by the time step adopted. In the present investigation, the desired numerical accuracy can be improved by reducing the CFL number, or equivalently by adding grid nodes to resolve a given wavelength while keeping the CFL value unaltered. In Figure 4, the enriched spatial resolution is achieved by changing the period of the wave from 1π to 2π, instead of doubling the number of nodes in space from 45 to 90. As a consequence, each wave will be resolved by 45 points in comparison to the previous 22, and the maximum numerical error at the same CFL value of 2 diminishes to a magnitude of 0.18 percent. In essence, if the TCI scheme has a suitable supporting mesh, a greater flexibility exists in temporal evolution of accurate numerical results. By virtue of the more favorable stability property than explicit schemes, the allowable time step of the implicit scheme depends only weakly on the mesh spacing. This particular property permits a wider time-step selection and perhaps will lead to a more efficient procedure for problem solving.

In Figure 5, the exact solution of the electrical field intensity and solutions from the SUE and TCI schemes are presented together for a CFL of 1.5. At this condition, the perfect shift does not prevail for the solution via the SUE method at the discontinous wave front (Fig 5a). Numerical solutions from the two methods indicate distinctive behavior at the singularity. The solution via the TCI method approaches the undisturbed field monotonically while the solution via the SUE method yields an oscillatory pattern near the finite jump. As the wave front passes through the numerical domain, the solution by the SUE method indicates a superior numerical accuracy over the solution by the TCI Scheme. The deviation from the exact result is less than 2-percent (Fig 5b).

The comparison of solutions of SUE and TCI schemes and the exact solution for a simple wave with a period of 2π and CFL of $2/\sqrt{3}$ is presented in Figure 6. The selected CFL value coincides with the theoretical limit of the SUE method in three dimensions. Again, numerical errors at the singular moving wave front are observed, but the numerical behavior of the
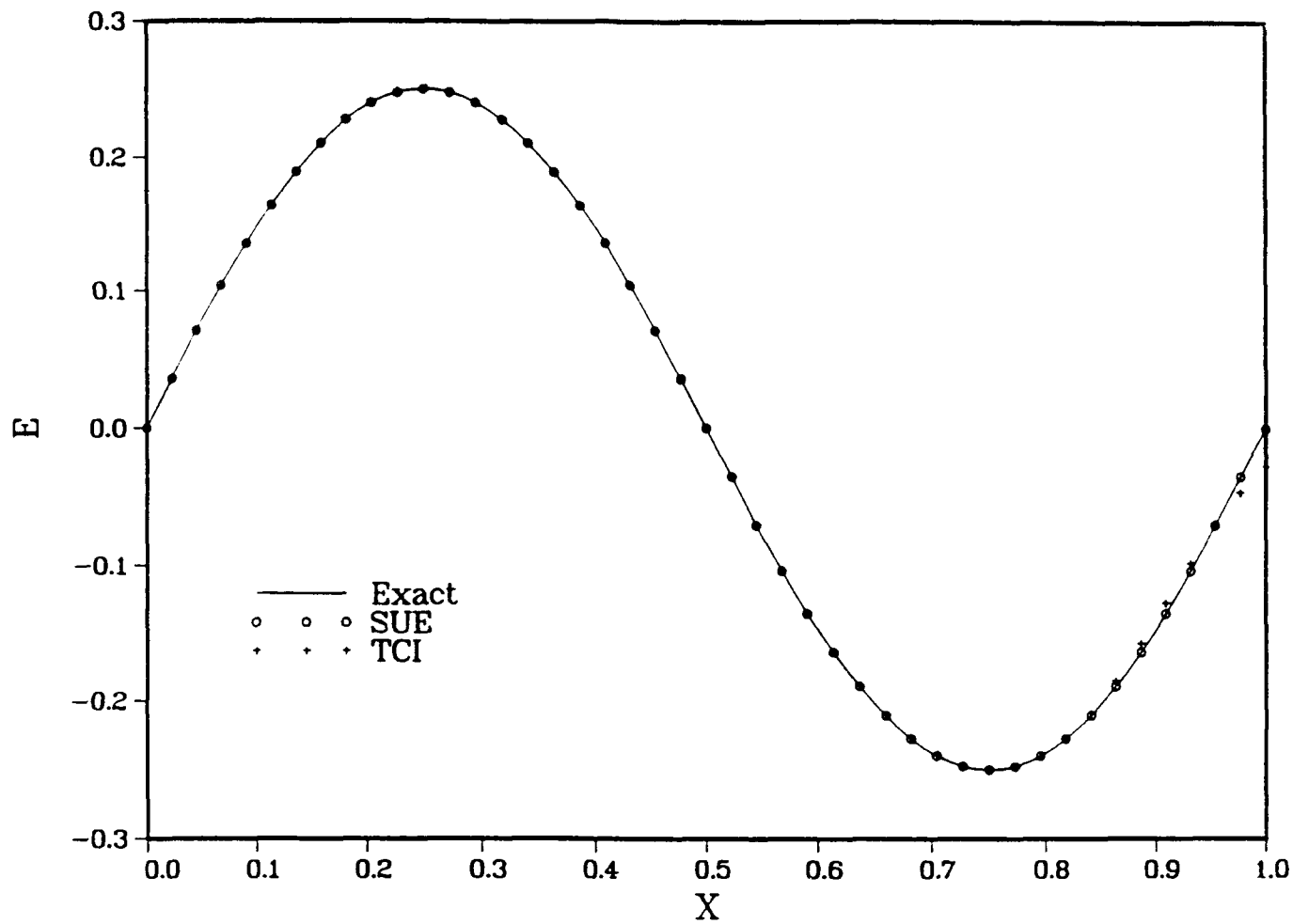
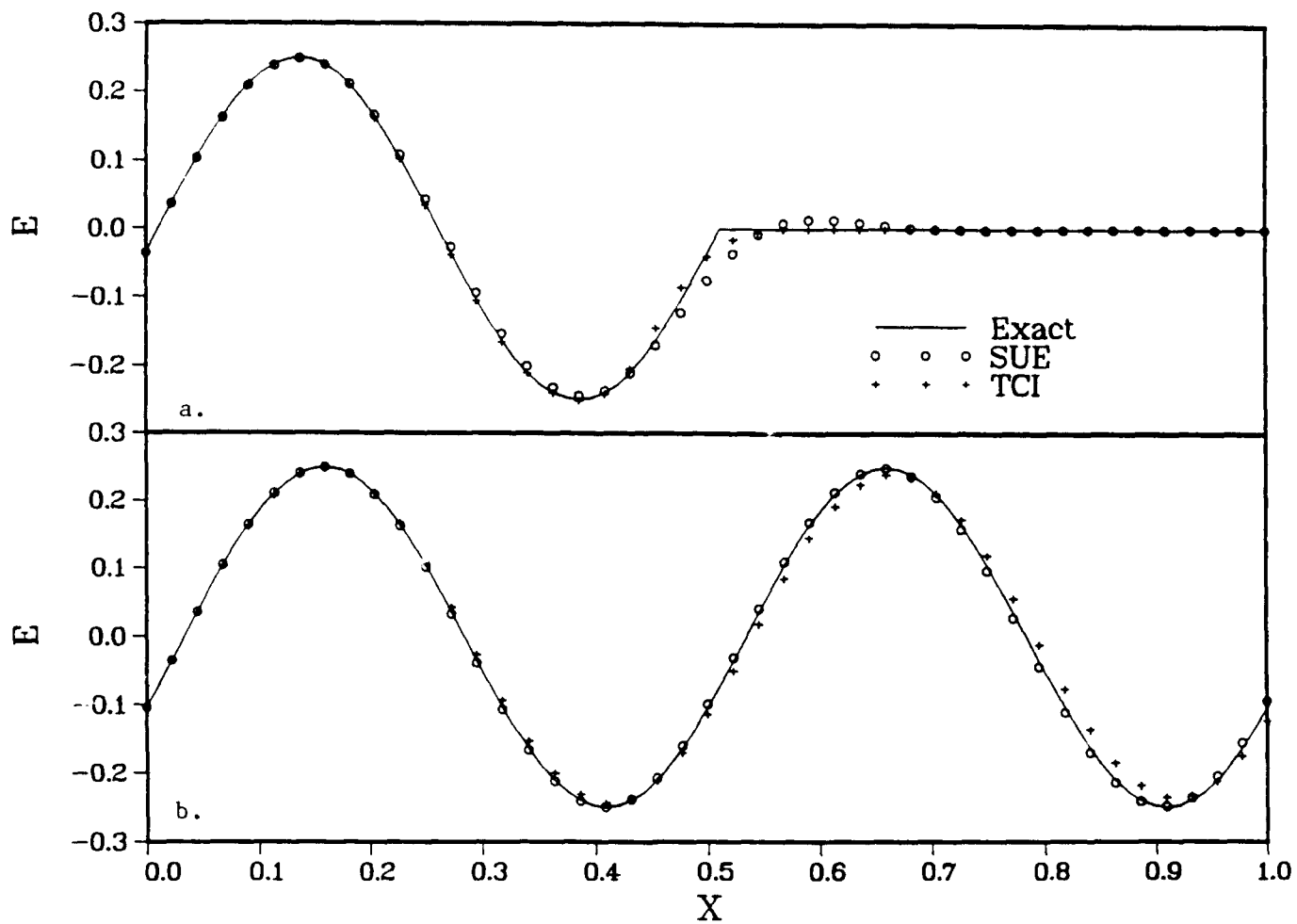Figure 4: Accuracy Dependence on Wave Number $CFL = 2.0$

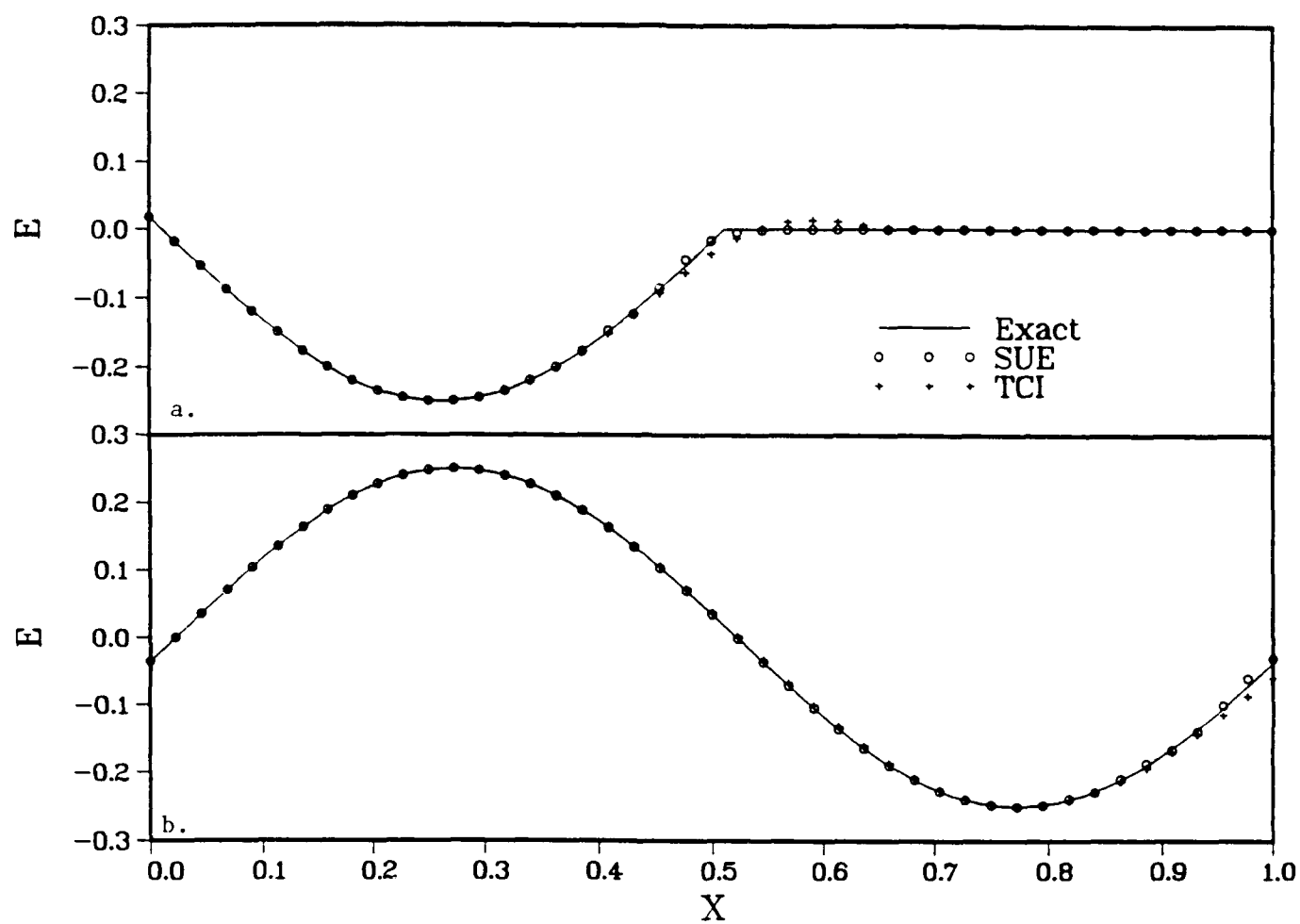Figure 5: Electrical Field Intensity $CFL = 1.5$

Figure 6: Electrical Field Intensity $CFL = 2/\sqrt{3}$

two methods is reversed. Now the SUE solution approaches the undisturbed electrical field monotonically and the TCI solution exhibits oscillations across the jump with a maximum normalized discrepancy of 5.5 percent (Fig 6a). In the entire domain downstream of the wave front, the numerical errors of both schemes are confined to a magnitude around a one-hundredth of one percent (Fig 6b). From these observations, the optimum application range of the TCI scheme for high numerical resolution electromagnetic simulation may reside within the CFL values above unity.

In Figure 7, for the first time, all numerical solutions developed in the present analysis are compared with the exact solution at a CFL of unity. For the trapezoidal inconsistent implicit (TII) scheme, this CFL value represents the maximum time step allowable from the stability analysis of a linear initial value system. Both solutions of the SUE and TII method possess the shift property and thus produce no numerical error at the moving wave front (Fig 7a). It may be of interest to note that the TII scheme is only one of a few implicit algorithms that can produce the simple wave solution with the shift property. The solution of TCI scheme alone shows numerical overshoot preceding and dissipative error trailing the moving wave front. As anticipated, solutions of the SUE and the TII schemes reached perfect accord with the exact solution in the complete solution domain (Fig 7b). The solution of TCI scheme underpredicts the amplitude of wave by a maximum of 1.7 percent and contains an identifiable leading phase error which has been verified by our earlier discussion of Figure 2.

The last comparison of all numerical solutions is depicted in Figure 8, where the CFL number is asigned a value of 0.75. At the discontinuous wave front, all numerical simulations exhibit oscillatory error across the jump. The numerical errors normalized by the exact wave amplitude span an extreme magnitude of 10.2, 10.9, and 13.4 percent respectively for the SUE, TII and TCI schemes (Fig 8a). In the postwave front region, the solutions by the SUE and TII schemes are nearly identical (Fig 8a). The largest error is again exhibited by

26

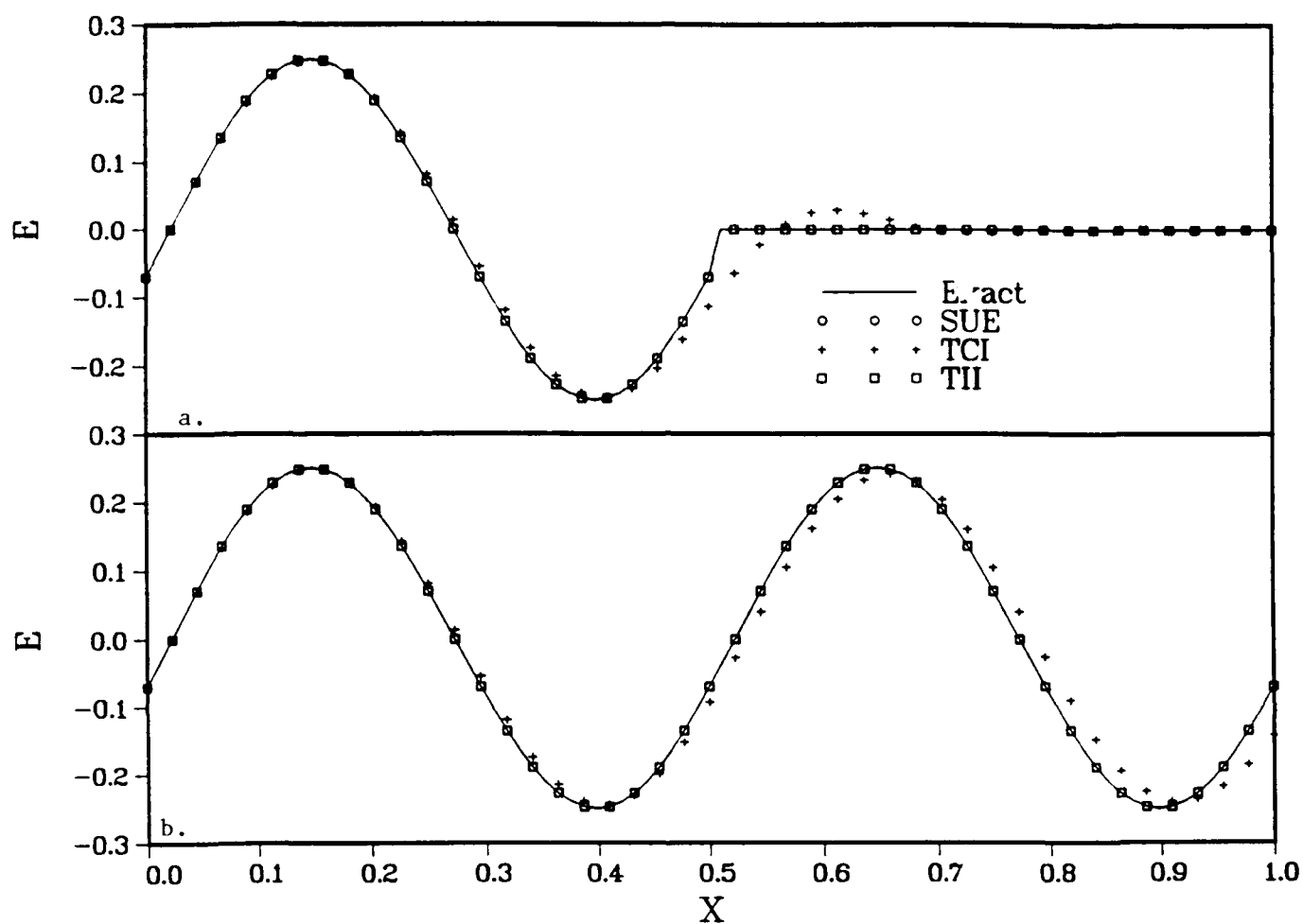# Electrical Field Intensity   CFL=1.0

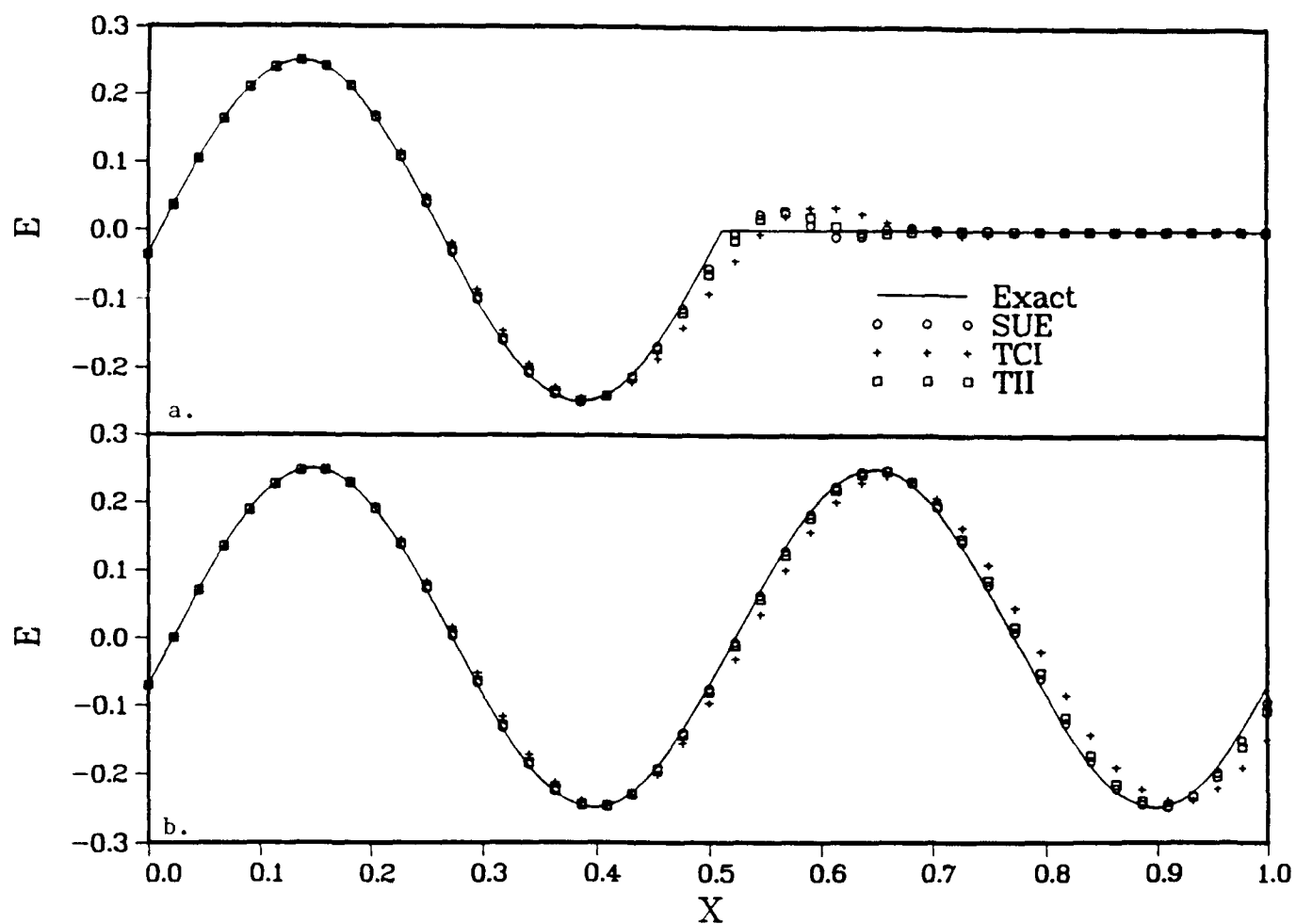Figure 7: Electrical Field Intensity $CFL = 1.0$

Figure 8: Electrical Field Intensity $CFL = 0.75$

the TCI scheme and amounts to less than 2 percent. However, one should note that the TCI scheme is not recommended in this range of CFL values in practical application. The newly developed trapezoidal consistent implicit procedure may be critical for improvement of numerical efficiency of electromagnetics simulation. Overall, the TCI scheme is easily the best choice for further development.

In the second group of numerical results, the three numerical procedures are compared for a propagating transverse wave at an angle of incidence to the coordinates. In all cases studied, the exact solution of the incident wave was used to overspecify numerical boundary conditions of the initial value system. Under this condition, the well-posedness issue may arise for the difference system[23]. The prescribed exact wave solution at the truncated boundaries may still appear as a perturbation to the difference system. The possibility of sustaining a continuous numerical solution by a wider class of perturbations to the initial data was assessed here. All solutions were evolved for more than a thousand time steps at a CFL of unity which corresponds to more than 22 cycles of a right-running wave. The implicit schemes are multiple-step methods which require additional intermediate temporal data at the computational boundary. The implementation of these intermediate temporal data at the numerical boundaries for implicit methods (TII and TCI) was also investigated. Figure 9 depicts a typical electrical field intensity of a traveling wave across the two-dimensional domain at 45 degrees with respect to the x coordinate (result of the TCI Scheme). Numerical solutions of the three schemes show comparable features and are nearly identical. In comparison with the first-order numerical procedure[7], no visible dissipative errors are observed along the wave crests.

In Figure 10, the L2 norms of calculated electrical field intensity of the SUE, TII, and TCI schemes are given. The maximum discrepancy of the L2 norm from the exact solution belongs to the SUE scheme with a magnitude of 0.014. The pattern of quasi-physical errors exhibits a symmetric structure with respect to the principal axis of wave motion
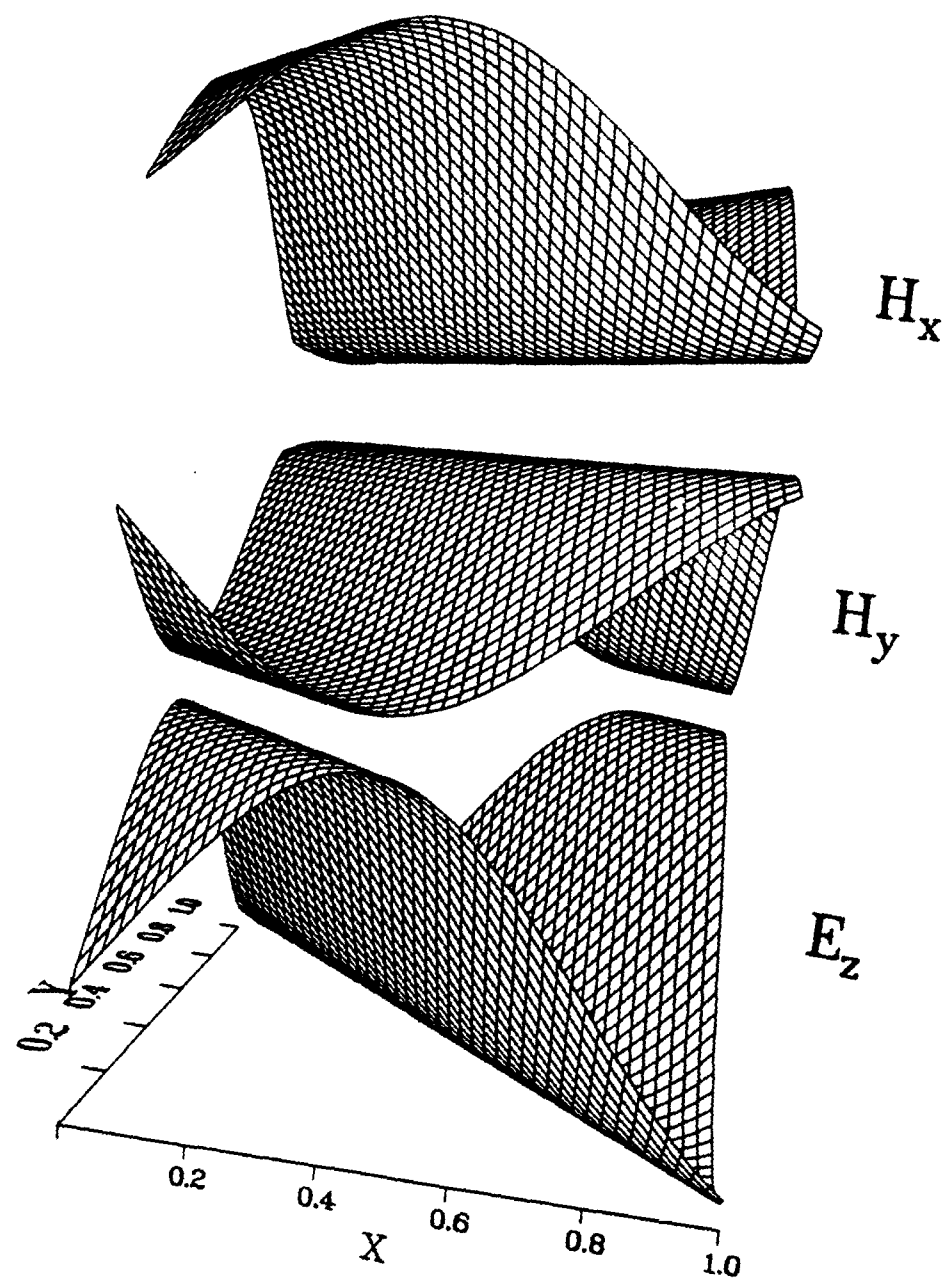
Figure 9: Transverse Electromagnetic Wave via Trapezoidal Consistent Implicit Scheme ($CFL = 2.0$, $p = 2\pi$, $\phi = 45°$)
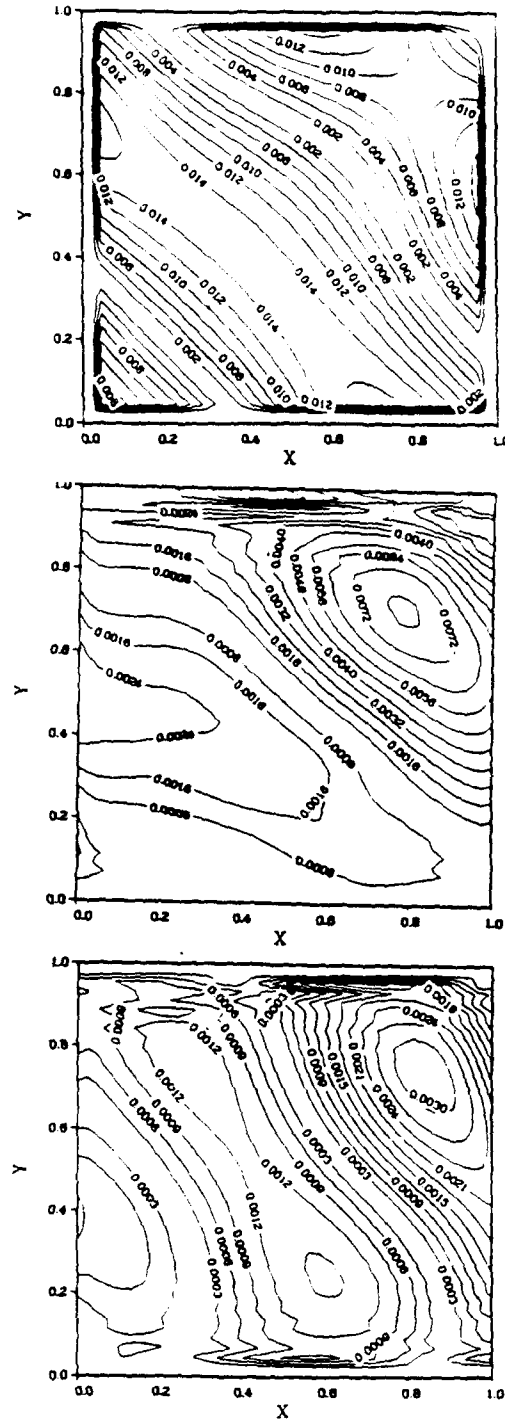
Figure 10: L_2 Norm of Electric Field Intensity ($CFL = 1.0$, $\phi = 45^\circ$) (a) SUE. (b) TH. (c) TCI.

and all errors are clustered adjacent to the numerical boundary (Fig 10a). Basically, the specification of the exact solution at the boundary appears as a perturbation and does not necessarily belong to the class of initial data for which the differential problem is well-posed. The solution via TH scheme yields a maximum L2 norm lower by one half to that of the SUE method (Fig 10b). The structure of numerical error is asymmetric to the principal axis of the wave propagation. However, a definitive attribution of this peculiar feature to either the artificial numerical boundary conditions or the numerical sweep bias is not certain at present. The numerical result generated by the TCI scheme contains the lowest error with the maximum L2 norm (0.0028) just a fifth of the SUE method. The distribution of quasi-physical error is similar to the two trapezoidal implicit methods as expected (Figs. 10b, 10c). Nominally, all numerical algorithms considered are second-order in time and space, but the subtle difference in numerical approximations for the TCI scheme has gained it a superior accuracy over the TH scheme in the two-dimensional calculation.

The effects of intermediate temporal data implementation for the approximate factored scheme on solution accuracy were isolated by carrying out two otherwise identical calculations with different data sets for the intermediate step. A right-running transverse wave inclined at 60 degrees to the x-axis was simulated by the TCI scheme. Numerical results were recovered by repeating the new time level data at both the first and the final numerical sweeps (Fig 11a), and by deriving the first sweep data from the final time level as indicated in our earlier discussion (Fig 11b). These results demonstrate that applying repetitively the next time level data for both factored sweeps has introduced greater errors than has applying the derived data near computational boundaries. The former procedure is commonly used in most computational fluid dynamics practices even for unsteady fluid dynamics phenomena[23]. Its impact on numerical stability and fidelity to physics in solving a time-dependent wave problem may be crucial. In addition, the intermediate solution from an approximate factored scheme is known to have no corresponding physical meaning
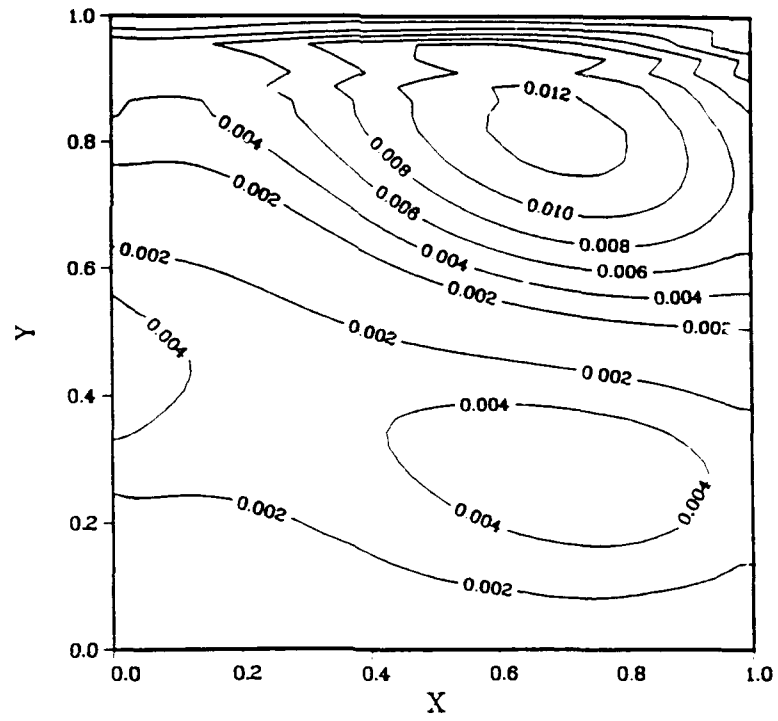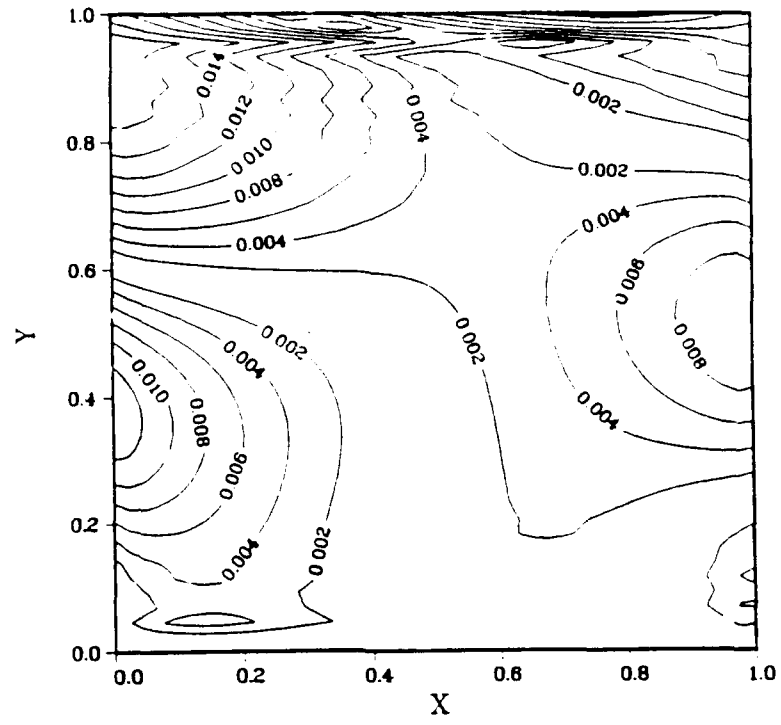
32

Figure 11: L_2 Norm of Electric Field Intensity with TCI Scheme ($CFL = 1.0$, $\sigma = 60^\circ$) (a) Repeating and (b) Derivative Data on Intermediate Step

which could be an undesirable feature of the present implicit procedures. A remedy for this shortcoming, if necessary, may require reverting the present implicit algorithm to the original alternating direction implicit formulation[28,30,31].

The last group of problems analyzed is the transverse electromagnetic wave induced by a point current source. Since an isotropic point source will generate a circular propagation pattern and the relatively sparse mesh point distribution at the point source is unable to provide sufficient numerical resolution[7,15], only the ability of solutions to retain the simple radiating wave pattern is investigated. The boundary conditions on the truncated computational domain require incoming eigenvectors (one-dimensional characteristics) to vanish in all directions. The one-dimensional characteristic boundary condition is the exact and well-posed condition for one-dimensional wave motion. When applied to multiple dimensional phenomena, it may degenerate to only first-order accuracy, depending on the orientation and intrinsic structure of the wave motion[7,12,13,14,15]. In present analysis, the characteristic boundary condition, which is an inherent and intended consequence of the flux-splitting formulation, was imposed on each coordinate direction. In this sense, this approach represents the worst possible scenario for solving the point source problem in which the radiating wave motion is described by a Cartesian system. Unfortunately, using the coordinate transformation to align with the principal axis of wave motion has to wait for further development. A typical numerical result using the TCI scheme is depicted in Figure 12. The z component of the electrical, and x, y components of the magnetic field intensities were projected on separated planes but maintained at the identical physical location. Since quantification of these computed results was not attempted, only general features of the results will be briefly mentioned. At the singular point, the current induces a polarized electrical wave moving radially with a nearly symmetrical front, whereas the two components of the magnetic field reveal a basically two-dimensional structure opposite in phase across the point source. The numerical results are similar to those of Anderson's
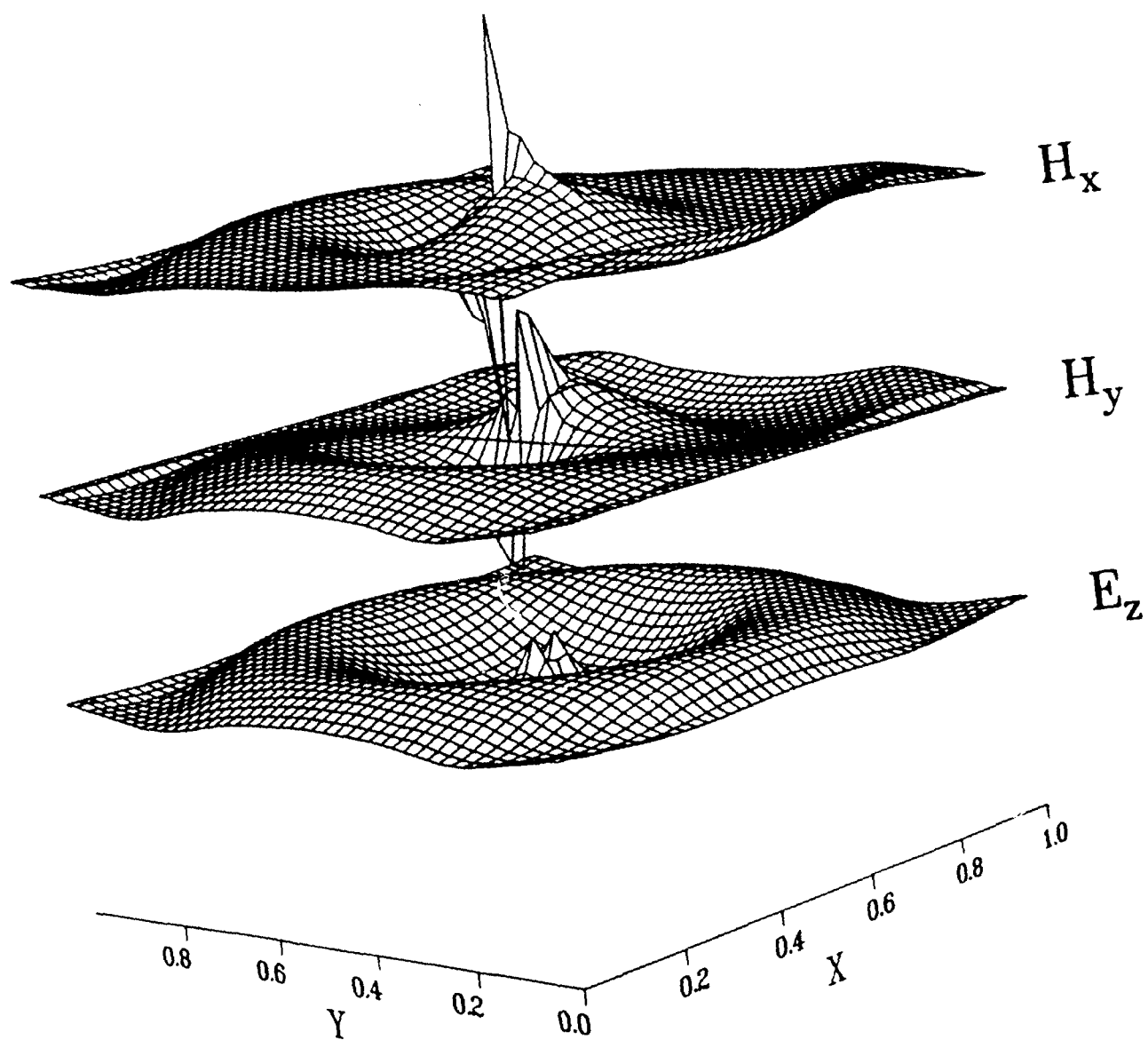
31

Figure 12: Electromagnetic Field Intensities with TCI Method (CFL = 2.0. $\rho=4\pi$)

calculation[7] and reproduce the features of the physics[14].

Calculated electrical field intensities by the SUE, TH, and TCI schemes are depicted in Figure 13. A monochromatic point source is designated at the midpoint of the computational domain (i,j = 23) with a normalized wave length of 2π and is switched on at the start of the numerical simulation. A total of 16 time steps were taken to allow the first electrical wave to pass through the truncated computational domain. Therefore, all given results are captured when the relatively sensitive trough of the wave front impacts upon the numerical boundaries. Like all previous one-dimensional calculations, each wave packet is resolved by 22 nodes. To compare the three numerical results on an equal footing, identical contour levels were used for the isodynamic plots. In general, all numerical simulations reveal similar wave structure in that all isodynamics form nearly concentric circles. Small differences in the wave structure are probably induced by relative phase errors of each individual solving scheme, but the most significant distortion of wave shape is recognized to be caused by the one-dimensional characteristic boundary conditions. The SUE method, being a single-step explicit method, produced a much better definition of the electrical pulsation at the point source. The specific behavior closely resembles the numerical result of Anderson on a 50 × 50 mesh system[7]. All implicit schemes tested here indicated a need for mesh refinement at the singular point. However, the TCI scheme seems to produce a less wave distortion than TH immediately adjacent to the truncated computational boundaries. In order to demonstrate the greater numerical efficiency of the TCI scheme, this procedure alone was applied to a pulsating point source problem at a CFL value of 2, which is unattainable by SUE and TH methods. The point source was moved to a corner of the calculation domain (10.10) and the transverse wave packet was still defined by 23 nodes in both coordinates. The numerical prediction of the electrical field intensity is displayed after an arbitrarily selected 120 time steps. The resolution at the point source appears to markedly improve but really is just highlighted by the denser contour levels (Fig 14). A
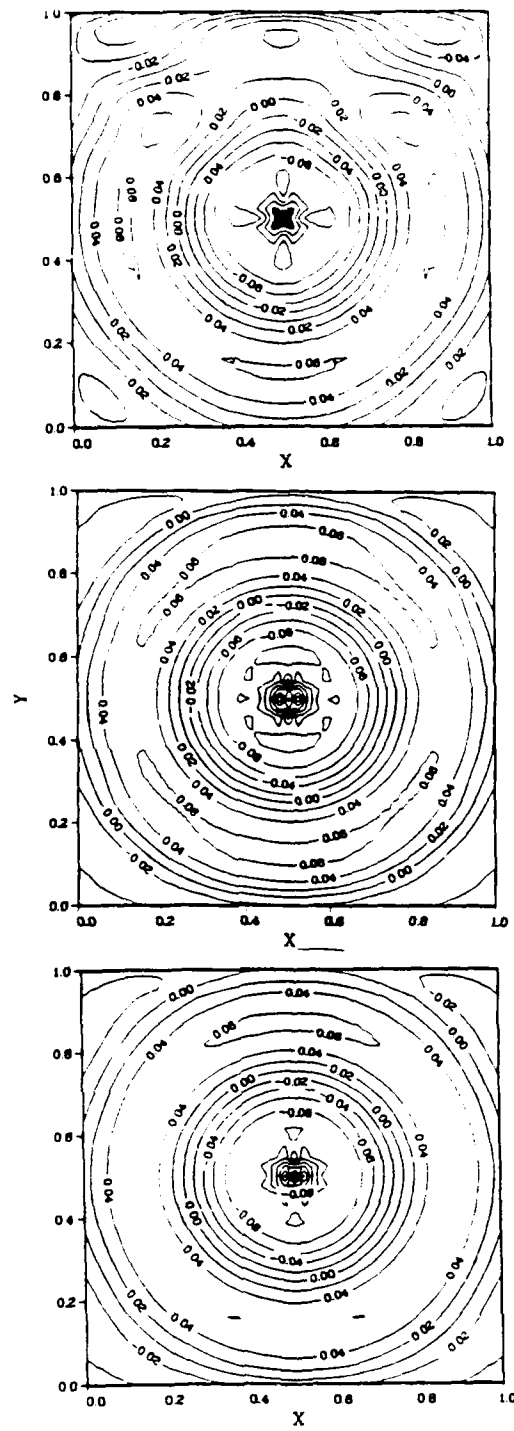
Figure 13: Isodynamics of Electric Field Intensity (CFL=1.0, p=4π)

quantative comparison with other known results has not been achieved at present[7,15]. The only conclusion one may offer is that the numerical results are consistent with the previous calculations depicted in Figure 13. The accumulated distortion of the radiating wave structure generated by the one-dimensional characteristic boundary conditions becomes more annoyingly pronounced on rectilinear coordinates. particularly. in view of the fact that the present formulation is designed to satisfy the exact one-dimensional characteristics and is capable of aligning the coordinates with the principal axis of wave motion. thus reducing the farfield to a one-dimensional problem. This observation reinforces the urgency to complete the incorporation of coordinate transformation into the new method.
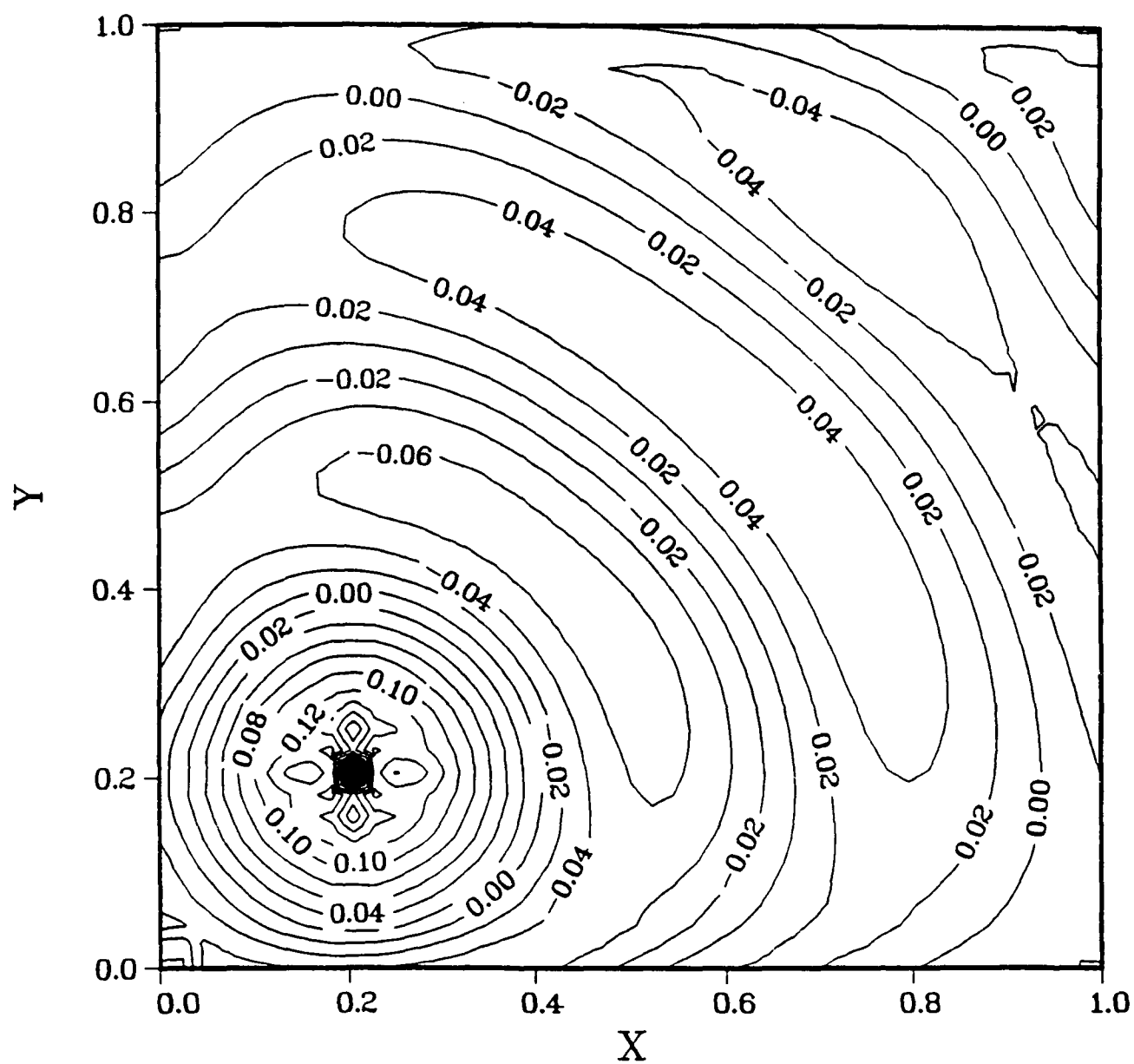
Figure 14: Isodynamics of Electric Field Intensity (CFL=1.0. TCI Scheme. p=4π)

5. Conclusion

New trapezoidal windward implicit schemes based on the flux splitting concept were successfully developed to solve the time-domain Maxwell equations. The trapezoidal consistent implicit scheme is unconditionally stable for the linear initial value system and provides a greater flexibility and numerical efficiency to numerically simulate electromagnetic wave phenomena. Applied to two-dimensional problems, the present implicit schemes generated solutions with an accuracy comparable to the established explicit method and allowed a greater time step size to describe the time-dependent wave phenomena.

The full potential of the present eigenvector formulation is still not fully explored until the general coordinate transformation is functional. By realignment of the coordinate to the principal wave motion, the eigenvector formulation will be enhanced by the exact and well-posed one-dimensional, no-reflecting characteristic conditions on truncated computational boundaries. In principle, the extension of the procedure to three-dimensional systems is possible but may not be straightforward. Effort is required to convert the present approximate factored scheme to the orginal ADI method for temporal accuracy.

6. References

1. Park. C.. "Assessment of Two-Temperature Kinetic Model for Dissociating and Weakly-ionizing Nitrogen." J. of Thermophysics and Heat Transf. Vol 2. No 1. Jan 1989. pp8-16

2. Shang. J.S. and Josyula. E.. "Numerical Simulations of Non-Equilibrium Hypersonic Flow Past Blunt Bodies." AIAA Preprint 88-0512. Jan.. 1988. Accepted by AIAA J for publication.

3. Candler. G.V. "On the Computation of Shock Shapes in Non-Equilibrium Hypersonic Flows." AIAA Preprint 89-0312. Jan.. 1989

4. Aftosmis. M.J. and Baron. J.R.. "Adaptive Grid Embedding in Non-Equilibrium Hypersonic Flow." AIAA Preprint 89-1652. June 1989

5. Bird. R.B.. Stewart. W.E.. and Lightfoot. E.N.. Transport Phenomena. John Wiley and Sons. Inc.. New york. 1960

6. Shankar. V.. Hall. W. and Mohammadian. A.. "A CFD-Based Finite-Volume Procedure for Computational Electromagnetics - Interdisciplinary Applications of CFD Methods." AIAA Preprint 89-1987. June 1989

7. Anderson. D.A.. "Interdisciplinary Applications of Simulation Computational Fluid Dynamics (CFD) and Radar Cross Section (RCS)." AFATL-TR-88-65. AF Armament Lab.. Eglin AF Base. FL.. April. 1988

8. Goorjian P.M.. "Algorithm Development for Maxwell's Equations for Computational Electromagnetism." AIAA Preprint 90-0251. Jan. 1990

9. Yee. K.S.. "Numerical Solution of Initial Boundary Value Problems Involving Maxwell's Equations in an Isotropic Media." IEEE Trans. Antennas Propagat. Vol AP-14. pp 302-307. May 1966

10. Taflove. A. and Umashankar. K.R.. "Finite-Difference Time-Domain (FDTD) Modeling of Electromagnetic Wave Scattering and Interaction Problems." IEEE Antennas Propaga-

tion Newsletter, April, 1988

11. Harrington, R. R. Time-Harmonic Electromagnetic Fields McGraw-Hill Book Co., New York, 1961.

12. Sommerfeld, A., Partial Differential Equations In Physics, Academic Press Inc. Publishers, New York, NY, 1949

13. Higdon, R., "Absorbing Boundary Conditions for Difference Approximations to the Multidimensional Wave Equation," Math. of Comp. Vol. 47, No. 175, 1986, pp 437-459

14. Enquist, B. and Majda, A., "Absorbing Boundary Conditions for the Numerical Simulation of Waves," Math. of Comp., Vol. 31, July 1977, pp. 629-651

15. Muir, G., "Absorbing Boundary Conditions for the Finite-Difference Approximation of the Time-domain Electromagnetic Field Equations," IEEE Trans. Electroma. Compat. Vol EMC-23, No. 4, Nov. 1981, pp.377-382

16. Steger, J.L. and Warming, R.F., "Flux Vector Splitting of the Inviscid Gasdynamics Equations with Application to Finite Difference Methods," J. Comp. Phys., Vol.40, No.2, Feb. 1987, pp.263-293

17. Van Leer, B. "Flux-Vector Splitting for the Euler Equations," Lecture Notes in physics, Vol. 170, 1982, pp. 501-512

18. Roe, P.L., "Characteristic-Based Schemes for the Euler Equations," Ann. Rev. Fluid Mech., Vol. 18, 1986, pp.337-365

19. Anderson, W.K. Thomas, J.L. and Van Leer, B., "A Comparison of Finite Volume Flux Vector Splittings for the Euler Equations," AIAA Preprint 85-0122, Jan. 1985

20. McMaster, D.L., Shang, J.S. and Gaitonde, D., "A Vectorized Gauss-Seidel Line Relaxation Scheme for Solving 3D Navier-Stokes Equations," AIAA Preprint 89-1948-CP, June 1989

21. Gaitonde, D. and Shang, J.S., "A Numerical Study of Viscous Shock-On-Shock Hypersonic Flows With a Modified Steger-Warming Flux Split Scheme," AIAA Preprint 90-1491,

June 1990

22. Kreiss. H. O.. "Initial Boundary Value Problems for Hyperbolic Systems." Common. Pure and Applied Math. XXII. 1970. pp. 277-298

23. Shang. J.S.. "An Assessment of Numerical Solutions of the Compressible Navier-Stokes Equations." J. of Aircraft. Vol. 22. No. 5. May 1985 pp. 353-370

24. Harten. A.. "On a Class of High Resolution Total-Variation-Stable Finite Difference Schemes." SIAM J. Num. Anal.. Vol 21. 1984. PP. 1-23

25. Yee. H.C.. "A Class of High-Resolution Explicit and Implicit Shock-Capturing Methods." NASA TM 101088. Ames Research Center. CA Feb. 1989

26. Godunov. S.K.. "A Finite Difference Method fo the Numerical Computation of Discontinuous Solutions of the Equations of Fluid Dynamics." Math. Sb.47 1959. pp. 357-393

27. Warming. R.F and Beam R.M.."Upwind Second-Order Difference Schemes and Applications in Unsteady Aerodynamics Flows." Proc. AIAA 2nd Computational Fluid Dynamics Conference. Hartford. CN. 1975. pp. 17-28

28. Warming. R.F. and Beam R.M.."On the Construction and Application of Implicit Factored Schemes for Conservation Laws." SIAM-AMS Proceedings. Vol. 11. 1978. pp. 85-129

29. Kutler. P. and Lomax. H.."The Computation of Supersonic Flow Fields about Wing-Body Combinations by Shock-Capturing Finite Difference Techniques." Lecture Notes in Physics. Vol. 8. Springer-Verlag. Berlin. 1971. pp. 24-29

30. Anderson. D.A.. Tannehill J.C.. and Pletcher. R.H.. *Computational Fluid Mechanics and Heat Transfer*. Hemisphere Publishing Corporation. McGraw-Ihil Book Co.. 1981

31. Briley W.R. and Mcdonald H.. "On the Structure and Use of Linearized Block Implicit Schemes." J. Comp. Phys. Vol. 31. No. 1. Jan. 1980. pp 54-73

List of Abbreviations and Symbols

$\bar{\bar{A}}, \bar{\bar{B}}, \bar{\bar{C}}$	coefficient matrices of the Maxwell equations
CFL	Courant-Friedrichs-Levy number
$\bar{\bar{D}}$	matrix of the eigenvalue
$\bar{E}$	electric field intensity
$\bar{F}, \bar{G}$	flux vectors of the Maxwell equations
$\bar{H}$	magnetic field intensity
i, j	indexes of the discretized spatial points
$\bar{\bar{S}}$	matrix of similar transformation
t	time
$\bar{U}$	dependent variables of the Maxwell equations
$\bar{\bar{W}}$	eigenvectors
x, y, z	Cartesian coordinates
ϵ	electric permittivity
λ	eigenvalue of coefficient matrices
μ	permeability
ξ, η, ζ	transformed coordinate system
ξ_x, ξ_y, ξ_z	metrics of coordinate transformation

superscripts

$+, -$	Variable associated with positive or negative eigenvalue respectively
$*$	Intermediate variable during numerical sweep
n	time level